Biogeosciences Discuss., doi:10.5194/bg-2015-629, 2016
Manuscript under review for journal Biogeosciences
Published: 18 January 2016

Biogeosciences Discussions Open Access EGU

Drainage reduces CO_2 uptake and increases CO_2 efflux by a Siberian floodplain due to shifts in vegetation community and soil thermal characteristics

M. J. Kwon[1*], M. Heimann[1,2], K. A. Luus[1,3], E. A. G. Schuur[4], N. Zimov[5], S. A. Zimov[5], M. Goeckede[1]

[1] Biogeochemical Systems, Max Planck Institute for Biogeochemistry, Jena, Germany

[2] Division of Atmospheric Sciences, Department of Physics, Helsinki University, Helsinki, Finland

[3] Dublin Institute of Technology, Dublin, Ireland

[4] Center for Ecosystem Science and Society, Department of Biological Sciences, Northern Arizona University, Flagstaff, USA

[5] North-East Science Station, Pacific Institute for Geography, Far-Eastern Branch of Russian Academy of Science, Chersky, Republic of Sakha (Yakutia), Russia

Correspondence to: M. J. Kwon (mkwon@bgc-jena.mpg.de)

Abstract. With increasing air temperatures and shifts in precipitation patterns forecasted in the Arctic over the coming decades, thawing of ice-rich permafrost is expected to change the hydrological conditions in large parts of the region by creating mosaics of wetter and drier areas. The objective of this study is to investigate how lowered water table depths of formerly wet floodplain ecosystems affect CO_2 fluxes measured with a closed chamber system, focusing on the roles of changes in vegetation community structure and soil thermal characteristics. We found that a decade-long drainage significantly increased the abundance of shrubs but decreased that of *Eriophorum angustifolium*, which subsequently made *Carex* species dominant. These two changes had opposing influences on photosynthetic uptake during the growing season: increased abundance of shrubs slightly increased gross primary production while replacement of *Eriophorum* by *Carex* significantly decreased it. Drainage also diminishes the heat capacity and thermal conductivity of soil, leading to increased soil temperatures in shallow layers during the daytime and decreased soil temperatures in deeper layers, and therefore reduced thaw depths. This soil temperature regime can intensify growing-season ecosystem respiration by up to

Biogeosciences Discuss., doi:10.5194/bg-2015-629, 2016
Manuscript under review for journal Biogeosciences
Published: 18 January 2016

93 % theoretically. Overall, drainage increased net CO_2 uptake (net ecosystem exchange) by 16 % over 20 days in 2013 but decreased it by 37 % over 66 days in 2014. During the frozen season, the drained transect emitted four times more CO_2 than the undrained transect. In summary, the net effect of these complex changes recently weakened net CO_2 uptake in the drained areas.

1 Introduction

Arctic ecosystems have long been known as large carbon sinks due to prevailing low air temperatures and the presence of permafrost. Although Arctic net primary production and standing biomass are smaller than that of adjacent climate zones (Saugier et al., 2001), the low decomposition rates of Arctic ecosystems have previously resulted in an accumulation ~1300 ± 200 Pg of belowground organic carbon (Hugelius et al., 2014). However, the tendency for Arctic ecosystem to take up more CO_2 on average than they release may be undergoing changes in the face of global climate change due to shifts in air temperature and precipitation patterns. While the photosynthetic rates and standing biomass in the Arctic have become larger (Epstein et al. 2012; Jia 2003; Myneni et al. 1997; Xu et al. 2013), so has the rate of organic carbon decomposition (Bond-Lamberty and Thomson, 2010), which has the potential to accelerate CO_2 cycle processes. However, it is not only a matter of how fast CO_2 circulates between the atmosphere and the upper soil layers, but also of what would happen to the massive amount of stored carbon that is currently stored in deeper permafrost layers. Thus, understanding how CO_2 flux patterns of the Arctic ecosystem change as a consequence of climate change and how this affects the fate of permafrost carbon is of great importance.

Gross primary production (GPP) is primarily determined by the length of the growing season and leaf area index (LAI), and is secondarily influenced by local climate conditions such as air temperature and soil moisture (Chapin et al., 2012b). With each plant species responding differently to changes in the aforementioned

Biogeosciences Discuss., doi:10.5194/bg-2015-629, 2016
Manuscript under review for journal Biogeosciences
Published: 18 January 2016

factors controlling GPP, and the possibility of successional changes in vegetation species distribution under a changing climate, the total amount of carbon assimilated (net primary production, NPP) and the rate of respiration (autotrophic respiration, R_a) may undergo complex changes. The rate of organic matter decomposition (heterotrophic respiration, R_h) increases under warmer and more aerobic conditions, and is also influenced by the quality of available organic matter. If any of these conditions are modified due to climate change, the rate of R_h can be altered in response.

Warming air temperatures have been observed in the Arctic (Serreze et al., 2000), and disproportionately warmer conditions are forecasted in response to climate change (Collins et al., 2013; Kirtman et al., 2013; Overland et al., 2014). The influence of temperature on CO_2 cycling processes in the Arctic has been well studied. As mentioned above, rates of both photosynthesis and organic matter decomposition have increased, and the continuing trends are predicted to change Arctic terrestrial ecosystems from a carbon sink to a source with accelerated organic carbon decomposition as dominant process (Koven et al., 2011; Schaefer et al., 2011). Schuur et al. (2015) predict that ~5 to 15 % of the permafrost carbon pool that corresponds to 120 ± 85 Gt of carbon (Schaefer et al., 2014) will be released to the atmosphere by 2100 under the current climate warming trajectory.

An increase in air temperature can closely influence soil hydrology and this may add complexity to CO_2 fluxes and the permafrost carbon pool. Atmospheric warming is usually followed by topographical changes and thus the formation of small-scale patches in hydrologic conditions on the ground: wetter conditions are generated in parts because thawed soil subsides (Jorgenson et al., 2006; O'Donnell et al., 2011) while the adjacent areas are drier when water laterally drains to subsided areas. These phenomena are particularly pronounced when increased air temperature thaws ice-rich permafrost, such as ice wedges and ice lenses. In some Arctic regions, changing precipitation patterns can aggravate or offset this situation. Precipitation in the Arctic has been generally increasing in recent decades (Kattsov and Walsh, 2000), but patterns are fluctuating yearly and spatially (Curtis et

Biogeosciences Discuss., doi:10.5194/bg-2015-629, 2016
Manuscript under review for journal Biogeosciences
Published: 18 January 2016

al., 1998; Stafford et al., 2000) and the surface water balance has also been found to be decreasing at times (Oechel et al., 2000). Increasing precipitation is expected in general in the Arctic because of intensified hydrological cycles under climate change, but the net effect can significantly vary by region (Bintanja and Selten, 2014; Huntington, 2006; Kirtman et al., 2013). Therefore, areas within the Arctic ecosystem can become heterogeneously wetter or drier by the combined effects of atmospheric warming and permafrost thaw, and varying rates of precipitation.

Several studies have investigated effects of drainage on CO_2 fluxes in the Arctic (Table 1). Field water table depth (WTD) manipulation experiments and comparison studies with varying WTD generally showed decreased net CO_2 uptake or increased net CO_2 emission at lowered water levels, primarily driven by increased ecosystem respiration (ER) (Christensen et al., 2000; Huemmrich et al., 2010; Kim, 2015; McEwing et al., 2015; Oechel et al., 1998; Olivas et al., 2010; Zona et al., 2011). In most cases GPP increased as well. Although some studies showed slightly increased net CO_2 uptake when the increase in GPP was larger than the increase in ER (Merbold et al., 2009; Natali et al., 2015), the magnitude of the increase in ER was usually larger than that of GPP in drier conditions (Christensen et al., 2000; Huemmrich et al., 2010; Kim, 2015; McEwing et al., 2015; Oechel et al., 1998; Olivas et al., 2010; Zona et al., 2011). Between-site variability of changes in net ecosystem exchange (NEE) presented in Table 1 can be attributed to differences in observation period, vegetation type, and intensity and duration of WTD changes in the specific studies.

Laboratory experiments showed inconsistent results as well: a decrease in WTD resulted in either decreased (Johnson et al., 1996), decreased or increased by soil type (Billings et al., 1982), or increased (Peterson et al., 1984) net CO_2 fluxes. These findings emphasize that the net effect of changes in WTD are a complex interaction of how specific soil and vegetation types respond to drier conditions. Therefore, although previous

Biogeosciences Discuss., doi:10.5194/bg-2015-629, 2016
Manuscript under review for journal Biogeosciences
Published: 18 January 2016

studies have shown that WTD reduction affects GPP and ER rates, the direction and significance of changes in net CO_2 cycling have been found to differ from ecosystem to ecosystem.

Most of the existing field observation and incubation studies (Table 1) focused on short-term effects of changes in WTD while effects of drainage at timescales of decades or more have rarely been studied. Also most of these studies were carried out in North America in spite of the fact that permafrost regions in Eurasia cover about twice the area, and also contain twice the amount of carbon compared to North America (Tarnocai et al., 2009).

As a continuation of a short-term analysis on hydrological manipulation in northeastern Siberia (Merbold et al., 2009), this study will provide results on how more than ten years of drainage affects ecosystem structure and CO_2 fluxes. By directly comparing CO_2 fluxes of a pristine region to those from the drained area, out results go beyond the description of the immediate disturbance effects and clearly point out differences in pristine and drained ecosystem properties that highlight how the disturbed area adapted to the persistently drier conditions. Our investigation is focused on shifts in vegetation community structure, soil temperatures and thaw depths (TD), and how these changes subsequently influence net CO_2 exchange and its component fluxes GPP and ER (Figure 1). In addition to the growing season, phenomena during the frozen season will be also described, which is unique researched in drying manipulation experiment.

2 Methodology

2.1 Site description

The study site is located in a floodplain of the Kolyma River near Chersky, Northeastern Siberia (also written as Cherskii or Cherskiy). The dominant vegetation species are *Carex* species and *Eriophorum*

Biogeosciences Discuss., doi:10.5194/bg-2015-629, 2016
Manuscript under review for journal Biogeosciences
Published: 18 January 2016

angustifolium (Appendix 1). An organic peat layer (15-20 cm) has accumulated on top of alluvial material soils (silty clay), and some organic peat materials can be found in alluvial layers due to cryoturbation.

Mean daily temperatures range between -40 °C in January and +13 °C in July (annual mean: -12 °C). Annual precipitation amounts to 220 mm, with half of it falling as rain in summer (based on 1980-2014 data in Chersky weather station, data retrieved from Reliable Prognosis). Snowmelt in the surrounding river basin usually results in a spring flood with increased WTD up to 50 cm above the soil surface in late May/early June, followed by a gradual decrease in WTD in the early growing season. After the receding of the flood waters, the primary water source is precipitation. An analysis of growing-season (June to September) air temperature and precipitation since 1980 revealed periodic fluctuations on timescales of *ca.* 5 years but no persistent longer-term trends (Appendix 2).

A drainage ditch with ~200 m diameter was constructed in fall of 2004 (Merbold et al., 2009), to drain water from the surrounding area into the nearest channel (Ambolikha). As a result WTD in this drained area is lowered by 20 cm on average and by up to 30 cm at the peak of the growing season compared to undrained areas (Merbold et al., 2009). Despite some short-term fluctuations following precipitation events and evapotranspiration, this difference in WTD continues until the onset of flooding in spring of the following year.

Starting summer 2013, the site was revisited to investigate the net impact of a decade-long hydrologic disturbance on this permafrost-affected floodplain. To investigate the decade-long impact of the hydrologic disturbance in the area affected by the drainage, we measured at two sites in parallel (Figure 2): a drained site (68° 36’ 47” N, 161° 20’ 29” E), and an undrained control site (68° 37’ 00” N, 161° 20’ 59” E) which is approximately 600 m away from the drained site and not effected by the drainage. Ten observation sites in each drained and undrained area were selected using a stratified systematic sampling method: we first prescribed 10 positions with 25 m intervals along the boardwalks, and then selected the final locations by considering

Biogeosciences Discuss., doi:10.5194/bg-2015-629, 2016
Manuscript under review for journal Biogeosciences
Published: 18 January 2016

representative vegetation groups from each location, and selecting specimens small enough to fit within flux chambers (Table 2, Figure 2). All sites were located within *ca.* 2 m of boardwalks to minimize disturbances.

In this study, we analyze observations from three field campaigns conducted in 2013-14: 3 weeks from 20 July 2013 and 10 weeks from 15 June 2014 for the growing season and 4 weeks from 1 November 2013 for the frozen season. We present general differences between the drained and undrained transects, and also consider high to low WTD gradients within the transects when necessary. These are labeled as drained(D)_high, drained_low, undrained(U)_high, and undrained_low hereafter, and one observation site from each group is chosen as the core site for more frequent observations (Figure 2).

2.2 CO_2 flux measurement

At each observation site a polyvinyl chloride (PVC) collar was installed permanently, covering 60 cm × 60 cm, and the chamber was placed on top of it while measuring fluxes. Sensors for air temperature, air humidity, air pressure and photosynthetically active radiation (PAR) are equipped on one side of the transparent chambers (60 cm cubic, made of 4 mm-thick plexiglass) and all parameters were measured in parallel with fluxes. These sensors, along with three small fans on a vertical pole attached in one of the corners for mixing the air inside, were placed in the opposite direction to the sun so that shade does not bias incoming solar radiation. CO_2 flux was measured with non-steady-state flow-through (closed dynamic) method using an Ultra-Portable Greenhouse Gas Analyzer (UGGA, Los Gatos Research, USA), and all data were recorded at 1Hz with a CR1000 data logger (Campbell, USA).

In addition to measuring NEE using the transparent chambers, in summer we also measured ER by covering the chamber with a tarp that is impermeable for incoming radiation. In winter we did not find significant difference between NEE and ER probably due to low temperature, low solar radiation, and snow cover limiting photosynthesis and measured NEE only. We restricted each flux measurement to two minutes maximum to

Biogeosciences Discuss., doi:10.5194/bg-2015-629, 2016
Manuscript under review for journal Biogeosciences
Published: 18 January 2016

minimize saturation effects – warming and pressurized effects – of chambers. In case of strong incoming radiation especially in summer when temperature was increasing more than 1 °C per minute, ice packs were placed on the collar rims inside the chambers to keep temperatures constant.

To calculate CO_2 flux from the observed changes in CO_2 concentrations ($[CO_2]$) within 2 minutes, median values of the $[CO_2]$ slopes was computed with bootstrapping, and fluxes (μmole m^{-2} s^{-1}) were calculated by taking into account air temperature, pressure, and the volume and area of chamber. Fluxes that fell out of the range of mean (of each season) ± 3σ (standard deviation) were removed as outliers. GPP and ER are expressed in positive values, indicating the amount of CO_2 assimilated and respired, respectively. NEE with negative values denote net CO_2 uptake by terrestrial ecosystem while the positive values denote net CO_2 emission to the atmosphere.

Fluxes were measured at 20 sites equally in 2013 for wide spatial coverage. In 2014 fluxes were measured at four cores sites more often than the others for higher temporal resolution. Although the core sites were chosen based on WTD category, dominant vegetation species of these sites were different as well due to the alterations in long-term WTD.

2.3 Vegetation community structure

In 2013 the vegetation community structure was investigated by harvest, using the same method at nearby location as in 2003 (Corradi et al., 2005). All living vegetation inside the 1 m × 1 m quadrat was harvested along the transects (N = 4 per transect). Collected vegetation was sorted by species, completely dried at 40 °C and subsequently weighed (g dry biomass m^{-2}). Based on the dry biomass, relative abundance of each species (%) was estimated. Data from 2003 as a part of TCOS Siberia project (Corradi et al., 2005) was used in this study as reference.

Biogeosciences Discuss., doi:10.5194/bg-2015-629, 2016
Manuscript under review for journal Biogeosciences
Published: 18 January 2016

In 2014, we applied a non-destructive point-intercept method with a 60 cm × 60 cm quadrat that was divided using a 10 cm × 10 cm sub-grid. We recorded the plant species that a laser pointer hit when pointing downward at each sub-grid intersection, and calculated the percentage of each species' cover (%). This analysis was performed within each observation site so that vegetation community structure of observation sites can be linked directly to CO_2 fluxes. The same analysis was carried out at a spot 10 m away from each observation site to investigate independently from observation sites because observation sites were selected with a stratified method (see section 2.1).

2.4 WTD, TD and soil temperature

WTD was measured during each flux measurement using percolated PVC pipes with 25 mm diameter installed at each observation site. WTD was described relative to soil surface, with values larger than 0 cm denoting water standing above the soil surface. TD was estimated by pushing a measuring pole into the ground. At every second site (at sites with even numbers) soil temperature probes were installed at 5, 15, 25 and 35 cm (Th3-s, UMS, Germany), and data was recorded while fluxes were measured.

To investigate the effect of soil temperature on R_h, we aerobically incubated soils at 0-15 and 15-30 cm depths at 15 °C and estimated the respiration rates. By assuming Q_{10} values of 2 as mean value from tundra ecosystem (Zhou et al., 2009), by taking the respiration rates of 0-15 cm layer 3 times greater than that of 15-30 cm layer (aerobic incubation at 15 °C, data not shown) and by considering soil bulk density of each layer, we estimated theoretic R_h rates of the top 0-15 cm and bottom 15-30 cm soil layers across temperatures. Average growing-season soil temperatures of the high- and the low-WTD sites by separating 0-15 and 15-30 cm depths were calculated, the corresponding R_h rates of each site of each soil layer were acquired from the theoretic respiration rates and bulk density, and the relative respiration rates between high- and low-WTD sites were compared.

Biogeosciences Discuss., doi:10.5194/bg-2015-629, 2016
Manuscript under review for journal Biogeosciences
Published: 18 January 2016

2.5 Data analysis and extrapolation

2.5.1 Statistical analysis

Spatial differences in WTD and TD of 2013 between the two transects were tested with an independent t-test. Permutational multivariate analysis of variance (PERMANOVA) was performed to compare vegetation community structure between the drained and the undrained transects of 2013 as well as that of the year 2003. Data from 2014 was not compared with that from 2003 due to different experimental method employed. A two-way analysis of covariance (ANCOVA) was carried out with WTD category (high- and low-WTD) and depth as independent variables to compare soil temperatures between WTD categories. Data from 2014 were divided into three sub-seasons to distinguish seasonal variability and to make it comparable with data from 2013: (1) June 15 – July 5, (2) July 6 – July 26 and (3) July 27 – Aug 20. Correlations between WTD and TD were tested by taking values from August each year to minimize the seasonality.

To see if vegetation group differentiated fluxes of 2013, all fluxes were aggregated by vegetation group and one-way analysis of variance (ANOVA) was performed for each vegetation group as an independent variable. When independent variables significantly influenced dependent variables, Tukey's post hoc test was applied. To find out if vegetation group and/or soil temperatures significantly affect frozen CO_2 fluxes, one-way ANOVA and multiple linear regressions were performed, respectively. In addition, a multiple linear regression analysis was performed to find additional major environmental drivers for cold season CO_2 fluxes. For multiple linear regression analysis, significant variables were defined based on BIC (Bayesian information criteria) and the best fit regression models were found with these selected variables based on the AIC (Akaike information criterion). All statistical analyses were performed with R (R Core Team, 2013).

2.5.2 Extrapolation of growing-season CO_2 fluxes

Biogeosciences Discuss., doi:10.5194/bg-2015-629, 2016
Manuscript under review for journal Biogeosciences
Published: 18 January 2016

To compare how each vegetation group or each WTD group responds to environmental changes without variability induced by temporal discrepancies in sampling, and to visualize the implications of these differences for net growing-season CO_2 uptake, CO_2 fluxes for each vegetation and WTD group were extrapolated throughout the growing-season observation period. To simulate CO_2 flux rates we adapted a satellite-data-driven CO_2 flux model, the Polar Vegetation Photosynthesis and Respiration Model (PolarVPRM), which calculates high-latitude NEE as the sum of -1 · GPP and ER (Luus and Lin, 2015).

$$GPP = (\lambda \cdot T_{scale} \cdot W_{scale}) \cdot FAPAR_{PAV} \cdot \left(\frac{1}{1+\frac{PAR}{PAR_0}}\right) \cdot PAR \quad \text{… Equation (1)}$$

$$T_{scale} = \frac{(T-T_{\min})(T-T_{max})}{(T-T_{\min})(T-T_{max})-(T-T_{opt})^2} \text{ … Equation (2)}$$

$$W_{scale} = \frac{a \cdot WTD}{WTD_{max}-WTD_{min}} + b \quad (0 < a < 1, a+b=1) \text{ … Equation (3)}$$

where λ is maximum light use efficiency at low light levels, and PAR_0 is half-saturation value of PAR. T_{scale} and W_{scale} are scaling variables ranging between 0 and 1 that reflect the influence of air temperature and water availability, respectively. The set of three parameters required for calculating T_{scale}, i.e. T_{min}, T_{max} and T_{opt} were set to 0, 40 and 20 °C according to literature in order to avoid parameter instability that would arise from fitting these parameters due to the strong positive correlations between T and PAR. $FAPAR_{PAV}$ is the fraction of PAR absorbed by the vegetation calculated from Moderate Resolution Imaging Spectroradiometer (MODIS) Enhanced Vegetation Index (EVI).

Unlike in regional scale estimates by PolarVPRM, site-level meteorological observations of air temperature (T) and PAR were used as inputs, which were taken from sensors installed in chamber system (for calibration) and from nearby meteorological towers (for temporal extrapolation). Additionally, ER was calculated as a Q_{10} function rather than a piecewise linear function, and the influence of water availability on photosynthesis

Biogeosciences Discuss., doi:10.5194/bg-2015-629, 2016
Manuscript under review for journal Biogeosciences
Published: 18 January 2016

(W_{scale}) was calculated based on WTD determined next to each observation site at the time of flux measurement, with an optimized scaling factor to obtain the best fits between $GPP_{modeled}$ and $GPP_{observed}$.

Both parameters (λ and PAR_0) were fitted empirically in R. PAR_0 was obtained from the curve fit between GPP and PAR measured with flux observations using the nonlinear least squares curve fitting in R, and λ was calculated as the slope of the linear regression of observed GPP, and of GPP calculated from Eq. (1) with an initial value of λ =1. GPP was estimated excluding PAR terms when no positive relationship between GPP and PAR was found. GPP was then computed half-hourly using linearly interpolated WTD and EVI, as well as half-hourly measured air temperature and PAR from the meteorological station.

ER was calculated using an empirical Q_{10} model.

$$ER = \alpha \cdot e^{k \cdot Temp} \quad \ldots \text{Equation (4)}$$

where Temp is air temperature. The two free parameters in this exponential relationship between ER and air temperature, α and k, were empirically calculated from chamber-based measurement of ER and T using nonlinear least squares curve fitting in R. Once these coefficients were calculated, ER was calculated at half-hourly intervals with continuously measured and half-hourly-averaged air temperature at meteorological station at each transect.

Parameter optimization and flux extrapolation were carried out across four core sites separately for the year 2014 while 10 observation sites of each transect were categorized into 3 vegetation groups and pooled for the year 2013, by taking into account only *Carex* Species, *Eriophorum Angustifolium* and shrubs when the relative abundance of each species exceeded 10 % (Table 2). The categorized vegetation groups of the drained transect were EriophorumShrub, CarexEriophorum and Carex whereas those of the undrained transect were CarexShrub, Eriophorum and EriophorumShrub. The period of extrapolation was selected from the beginning to

Biogeosciences Discuss., doi:10.5194/bg-2015-629, 2016
Manuscript under review for journal Biogeosciences
Published: 18 January 2016

the end of observation time each year because WTD (W_{scale}) was not measured continuously beyond this period. The discrepancies between the observed and modeled fluxes were calculated with root mean squared error (RMSE) and mean bias error (MBE). All data points that were used for calibration were utilized for the error estimates due to the limited number of data points.

Uncertainty ranges of parameter fits were calculated using cross validation, by creating 2000 data subsets which consisted of randomly selected data points (bootstrapping, 80 % of the total dataset). For ER, mean and standard deviation of the 2000 resulting pairs of parameters were computed, subsequently for each 1 °C temperature bin, mean ER ± 2σ standard deviation was estimated to get error range. Similarly, mean and standard deviation of PAR_0 and λ were estimated for binned PAR, the range of GPP was subsequently estimated by including the other terms of Eq. (1). Low uncertainty ranges imply that variations in ER and GPP are mainly explained by air temperature and PAR, respectively. Because NEE is calculated as the sum of GPP and ER, uncertainty ranges were also determined by adding two error ranges. For sites where the number of data points is not enough to produce uncertainty ranges, the bootstrapping step was skipped.

3 Results

3.1 Drainage impact on WTD

During the three weeks in summer 2013 when flux observations took place, mean WTD remained at a constant level with only minor fluctuations over time due to evapotranspiration and rainfall. Average differences in WTD between the two transects were found to be significant (independent t-test, $P < 0.001$, $t = -4.55$, $df = 17.91$) with a mean drop of approximately 20 cm, and a maximum difference of up to 30 cm as a consequence of drainage (Figure 3a). Approximately the same difference in the mean WTD was observed in the middle of growing season of 2014; however, several significant rainfall events from late July of this year triggered WTD to increase in the low-WTD sites, especially in the drained transect (Figure 3b). Similar patterns were also observed

Biogeosciences Discuss., doi:10.5194/bg-2015-629, 2016
Manuscript under review for journal Biogeosciences
Published: 18 January 2016

in 2005, one year after the drainage ditch was installed (Merbold et al., 2009), implying that reductions in WTD with respect to the drained transect can be subject to strong variability, depending on rainfall patterns. Nonetheless, WTD difference between high and low sites showed distinct patterns.

3.2 Changes in ecosystem properties following drainage

3.2.1 Vegetation community structure

In the natural, undisturbed state, the vegetation community of this floodplain was dominated by *Eriophorum Angustifolium*, followed by *Carex* species, such as *appendiculata* and *lugens*, tussock-forming sedge (Appendix 1). These conditions were reflected in the observations from the year 2003 (Corradi et al., 2005), i.e. before the drainage ditch was constructed (Figure 4, top panel) as well as in the undrained transect in 2014 (Figure 4, center panel). After a decade of drainage, the abundance of shrubs (*Betula exilis* and *Salix* species, such as *fuscescens* and *pulchra*) in the drained transect increased significantly while that of *Eriophorum* decreased (Figure 4, lower panel). With the retreat of *Eriophorum*, *Carex* and shrubs became the dominant species (Figure 4, lower panel). In the undrained transect the vegetation community structures of the high- and the low-WTD sites were distinctively different with the dominant species of *Eriophorum* and *Carex*, respectively, but the drained transect had some areas with a transition stage. In the low-WTD sites of the drained transect where *Carex* and *Eriophorum* were dominant, a mixture of young *Carex* without discrete tussock forms or small developing tussocks and short and thin *Eriophorum* were observed.

Vegetation community structures in 2003 and in the undrained transect of 2013 were not statistically different (PERMANOVA, $F = 1.62$, $P = 0.19$) while significant differences were found between 2003 and the drained transect of 2013 (PERMANOVA, $F = 3.31$, $P < 0.05$) and also between the two transects of 2013 (PERMANOVA, $F = 5.22$, $P < 0.05$). Although we did not experimentally compare the two observation methods

Biogeosciences Discuss., doi:10.5194/bg-2015-629, 2016
Manuscript under review for journal Biogeosciences
Published: 18 January 2016

(see section 2.3), a qualitative comparison of results from 2013 (harvest) and 2014 (point intercept) showed similar abundance of each species.

The reported abundance of shrubs (*Betula* and *Salix* species) at the observation sites which was estimated in the 2014 with the point-intercept method may be underestimated especially in the drained transect since tall shrubs were excluded when selecting observation sites in order to make sure all vegetation could fit into the chambers when measuring fluxes (Note that these results are to compare CO_2 fluxes by vegetation group and are separate from those described in the previous paragraphs, see section 2.3)

3.2.2 Soil temperature and TD

The general trends observed across the two transects indicate that drainage resulted in stronger diurnal fluctuations in shallow layer soil temperatures, but colder deep layer soil temperatures compared to the high-WTD sites (two-way ANCOVA, Table 3 & Figure 5). It emphasizes the important role of water content for the thermal properties of soils. Soils at shallow layers tend to heat up more during the daytime at dry sites because of reduced heat capacity of dry soil. At the same time, these dry soils have lower thermal conductivity, so that the energy was not transferred downwards, and deeper layers remain colder than their counterparts at high-WTD sites. This mechanism affected TD, with the overall trend that low-WTD sites ended up with shallower TD later in the growing season (Figure 6). The positive correlations between WTD and TD were shown in correlation analyses (for 2013: $r = 0.47$, $P < 0.05$, for 2014: $r = 0.67$, $P < 0.001$).

3.3 Spatial and temporal variability in growing-season CO_2 flux rates

3.3.1 Vegetation effects on CO_2 fluxes

Chamber-based CO_2 flux measurements during the growing season of 2013 showed similar mean and standard deviation of NEE, GPP and ER rates between the two transects (Figure 7). However, fluxes showed

Biogeosciences Discuss., doi:10.5194/bg-2015-629, 2016
Manuscript under review for journal Biogeosciences
Published: 18 January 2016

large variability across observation sites within the transects of *ca*. 225 m, which was found to be closely linked to the dominant vegetation groups (Figure 7b, one-way ANOVA, NEE: $F = 24.99$, $P < 0.001$, GPP: $F = 11.23$, $P < 0.001$, ER: $F = 3.63$, $P < 0.01$). As a general trend, *Eriophorum*-dominated sites in both transects had larger rates of photosynthetic uptake than *Carex*-dominated sites, with the GPP rates of Eriophorum and EriophorumShrub greater than Carex, CarexEriophorum and CarexShrub by 17 to 39 % (Figure 7b). EriophorumShrub of the undrained transect had 4 % more GPP than Eriophorum but the difference was not significant (Figure 7b). EriophorumShrub within the drained transect had the largest CO_2 sink strength (the most negative NEE) while CarexEriophorum (drained) and CarexShrub (undrained) showed the lowest net uptake (Figure 7b). ER also differed by dominant vegetation group but as shown in Figure 7b the difference was not as pronounced as in GPP especially in the drained transect (Figure 7b). Because vegetation group was identified as a dominating controlling factor on CO_2 flux rates, extrapolation of fluxes as presented in the section 3.4.2 was carried out by pooling fluxes for each vegetation group.

Core sites were selected based on the WTD group but different WTD regimes resulted in variations in dominant vegetation groups, with high-WTD sites dominated by *Eriophorum* and low-WTD sites by *Carex* (Table 2). Although the rates of NEE, GPP and ER started at low levels in the beginning of the growing season and were enhanced in the middle of growing season as air temperature, PAR and plant biomass increased, variations by vegetation type were similar to those in 2013: drained_high (EriophorumShrub) showed the highest CO_2 uptake (the most negative NEE) over the growing season, and undrained_high (EriophorumShrub) followed as the second while both drained_low (CarexEriophorum) and undrained_low (CarexShrub) showed the lowest uptake (Figure 8).

3.3.2 Soil temperature effects

Biogeosciences Discuss., doi:10.5194/bg-2015-629, 2016
Manuscript under review for journal Biogeosciences
Published: 18 January 2016

ER was positively correlated with soil temperatures at 5 cm in all sites, but showed different rates and responses to temperature when grouped into WTD categories: the low-WTD sites showed higher or similar ER than the high-WTD sites across all temperatures and the corresponding gradients for the low-WTD sites were steeper in both transects compared to those of high-WTD sites (Figure 9). The average ER rates of the low-WTD sites were 7 – 27 % and 9 – 63 % higher than those of the high-WTD sites in 2013 and 2014, respectively (Figure 9).

When only soil temperature effects on R_h were considered based on the results from an aerobic incubation experiment, higher soil surface temperatures of the low-WTD sites increased R_h by 236 % whereas lower deep soil temperatures decreased it by 0.2 % compared to the high-WTD sites. Combining these two effects, R_h rates in drained areas were elevated by 93 % because of larger effects of the soil surface temperatures on compacted soils.

3.4 Gap-filled CO_2 flux time series

3.4.1 Model error

Comparing observed against modeled flux rates for all individual measurements in the database, the mean RMSE of ER was 0.6 and 0.8 μmole-CO_2 m^{-2} s^{-1} for 2013 and 2014, respectively, and that of GPP was 1.5 and 2.2 μmole-CO_2 m^{-2} s^{-1} for 2013 and 2014, respectively (Table 4). The undrained transect in 2013 showed generally lower RMSE and MBE compared to the drained transect (Table 4). Larger RMSE and MBE in the drained transect can be attributed to pooling of data points according to vegetation group as well as the limited number of data points: large error in GPP of the Carex group of the drained transect is from varying standing biomass and that of the EriophorumShrub of the drained transect is from the small number of data points. For the year of 2014, data points of each group came from a single site but varying WTD and thickening thaw depth over the growing season resulted in relatively large errors (Table 4).

Biogeosciences Discuss., doi:10.5194/bg-2015-629, 2016
Manuscript under review for journal Biogeosciences
Published: 18 January 2016

The PAR terms were excluded when fluxes of CarexEriophorum of the drained transect were interpolated because plotting GPP against PAR sorted by vegetation group indicated that GPP rates increased with increasing PAR in all but CarexEriophorum of the drained transect (Figure 10). This site showed slightly decreasing GPP with increasing PAR in relatively dry year of 2013, implying high PAR and air temperatures induced water stress that had a net effect of suppressing photosynthesis, rather than enabling photosynthesis, under very warm and sunny conditions.

3.4.2 Growing-season CO_2 fluxes

The modeled fluxes of both years showed the same general patterns as observed fluxes: *Eriophorum*-dominated sites showed higher GPP flux rates than *Carex*-dominated sites in both transects (Table 5), and high-WTD sites showed stronger CO_2 uptake than low-WTD sites (Table 5). The cumulative NEE range of the drained transect was -5 to -2 mole-CO_2 m^{-2} while that of the undrained transect was -3 to -1 mole-CO_2 m^{-2} over 20 days in 2013, and if the average CO_2 fluxes are calculated by weighing the proportion of vegetation group within the transects, drained transect showed 0.3 mole-CO_2 m^{-2} more CO_2 uptake over 20 days in 2013 (Table 5).

For 2014, the order of sink strengths was similar to that of 2013 data with the same vegetation group: drained_high (EriophorumShrub) had the strongest CO_2 uptake, followed by undrained_high (EriophorumShrub), drained_low (CarexEriophorum) and undrained_low (CarexShrub) (Table 5). The NEE range of the drained transect was -18 to -6 mole-CO_2 m^{-2} while that of the undrained transect was -13 to -9 mole-CO_2 m^{-2} over 66 days in 2014, and if the average CO_2 fluxes are calculated by weighing the proportion of WTD groups within the transects, drained transect showed 4.4 mole-CO_2 m^{-2} less CO_2 uptake over 66 days in 2014 (Table 5).

3.5 Frozen-season CO_2 flux rates

Biogeosciences Discuss., doi:10.5194/bg-2015-629, 2016
Manuscript under review for journal Biogeosciences
Published: 18 January 2016

Due to low air temperature, solar radiation and plant activity, CO_2 fluxes in the frozen season consisted only by respiration. The drained transect emitted four times more CO_2 compared to the undrained one on average, and some sites with *Eriophorum* showed sporadically high fluxes, the amount of which was comparable to ER of the growing season (Figure 11). On the other hand, the undrained transect did not show sporadic high fluxes in any of the observation sites (Figure 11). If this flux pattern is constant throughout November, the net CO_2 emission of this month can be 0.9 mole-CO_2 m^{-2} in the drained transect and 0.2 mole-CO_2 m^{-2} in the undrained transect. Vegetation group significantly affected CO_2 fluxes in the drained transect with higher fluxes in the presence of *Eriophorum* despite high variability (one-way ANOVA, $F = 6.31$, $P < 0.01$). Soil temperatures significantly influenced CO_2 fluxes in the drained transect but correlations were weak (multiple linear regression, adj. $R^2 = 0.39$, $P < 0.001$; Tsoil at 5cm, $P < 0.001$; Tsoil at 15 cm, $P = 0.93$; Tsoil at 5 cm × Tsoil at 15 cm, $P < 0.001$). The undrained transect was significantly affected by neither vegetation group nor soil temperatures possibly due to low variability. Multiple linear regression analysis revealed that soil temperatures, air pressure and abundance of *Eriophorum* influenced CO_2 fluxes significantly (multiple linear regression, drained transect: adj. $R^2 = 0.46$, $P < 0.001$; pressure, $P < 0.001$; Tsoil at 5 cm, $P < 0.001$; *Eriophorum*, $P < 0.001$; pressure × Tsoil at 5 cm, $P < 0.001$; pressure × *Eriophorum*, $P < 0.001$, undrained transect: adj. $R^2 = 0.21$, $P < 0.001$; Tsoil at 5 cm, $P < 0.01$; Tsoil at 15 cm, $P < 0.01$; Tsoil at 25 cm, $P < 0.01$; *Eriophorum*, $P < 0.05$; Tsoil at 5 cm × *Eriophorum*, $P < 0.001$; Tsoil at 15 cm × *Eriophorum*, $P < 0.001$; Tsoil at 25 cm × *Eriophorum*, $P < 0.001$).

4 Discussion

4.1 WTD changes from drainage

After flooding from snowmelt in the early growing season, the drainage ditch effectively lowered WTD by 20 cm on average in the drained transect. However, at the end of the growing season WTD in the low-WTD sites increased dramatically especially in the drained transect due to precipitation. The amount of precipitation

Biogeosciences Discuss., doi:10.5194/bg-2015-629, 2016
Manuscript under review for journal Biogeosciences
Published: 18 January 2016

was similar at both transects but WTD of the drained transect was more susceptible to change compared to the undrained transect because of the topography. Low WTD of undrained_low was from higher topography relative to the surrounding by *ca.* 30 cm so that precipitation was drained to the surrounding area, making WTD of this area constantly low. On the other hand low WTD of drained_low is solely from drainage ditch, and precipitation in this even terrain height rose WTD easily. In addition, active *Eriophorum* and some aquatic plants within the ditch area could hold water and delay water drainage at the end of growing season, which was different from the early growing season when vegetation was not effective enough. When ice-rich permafrost thaws and drains water, however, water drainage will be more effective than drainage manipulation of this study because thawing permafrost will induce topographical changes like in the undrained transect.

When water drains in a floodplain ecosystem, soil changes from anaerobic to aerobic condition, and consequently, vegetation community structure and soil temperatures (subsequently thaw depth) are altered. This alteration and following changes in CO_2 fluxes will be discussed further in detail, which direction each component goes and whether the drainage acts as moderate aerobic environment or as water stress.

4.2 Vegetation effects on GPP and carbon accumulation

Vegetation community structure was shifted toward *Carex* species and shrub species became more dominant while *Eriophorum* died out upon drainage. Observation sites represented this vegetation change from *Eriophorum* to *Carex.*

Changes in vegetation significantly altered GPP. Firstly, a greater abundance of shrubs increased GPP by 4 %. An increase in shrub prevalence resulted in slight increases in GPP in this study. This difference is expected to be larger for the region as net primary production (NPP) of the Arctic ecosystems increases with the abundance of shrubs (Shaver and Jonasson, 2001). There are many other factors to be considered when it comes to productivity but generally shrubs assimilate a larger amount of carbon than sedges, so GPP will increase in the

Biogeosciences Discuss., doi:10.5194/bg-2015-629, 2016
Manuscript under review for journal Biogeosciences
Published: 18 January 2016

drained area with larger shrubs included. Increasing abundance of shrubs not only changes carbon exchange rates between atmosphere and terrestrial ecosystem, but also carbon storage patterns in the ecosystem. In the drained transect living biomass – the sum of leaf and stem – was higher than in the undrained transect and in 2003, but with lower green leaves and higher stems mostly due to increased abundance of shrub species (Appendix 3). When shrubs continue to expand, a large portion of carbon will be stored in plants especially in shrubs' stems and the amount of litter added to soil – dead – will decrease (Appendix 3).

The second phenomenon was decreasing abundance of *Eriophorum*, causing *Carex* to become the dominant species. GPP of *Eriophorum*-dominated sites was significantly higher than that of *Carex*-dominated sites, thus decreasing *Eriophorum* reduced carbon accumulating in terrestrial ecosystem. Especially CarexEriophorum sites in the drained transect, which have been undergoing vegetation transition, showed even significantly lower GPP than other *Carex*-dominated sites. In this transition stage, vegetation assimilates a lower amount of CO_2 and can be susceptible to external disturbances. For instance, these sites showed slightly decreasing GPP with increasing PAR in the relatively dry year of 2013, implying high PAR most likely along with high air temperature caused water stress to plants. This transition stage effect cannot be trivial considering that the fraction of these areas is not small (3 out of 10 observation sites) and 10 years was not sufficient for plants to stabilize in a new, drier condition. CarexShrub in the undrained transect, which can be considered as the potential vegetation community of drained_low sites, showed higher GPP than CarexEriophorum and increasing GPP with higher PAR in both years, implying CarexEriophorum sites will take up more amount of CO_2 and do not undergo water stress as easily as now. However, they still showed lower GPP than *Eriophorum*-dominated high-WTD sites especially in 2013 when precipitation was lower, thus drainage can limit vegetation activity, and carbon assimilation.

Biogeosciences Discuss., doi:10.5194/bg-2015-629, 2016
Manuscript under review for journal Biogeosciences
Published: 18 January 2016

In this study, the effects of decreasing *Eriophorum* were larger than those of increasing shrub prevalence, which could be due in part to underestimates in shrub's abundance and challenges in predicting how CO_2 uptake may increase with increasing shrubs with given results. However, given that CarexShrub sites in the undrained transect has lower CO_2 uptake rates than *Eriophorum*-dominated sites in the same transect, drainage and subsequent changes in vegetation can weaken CO_2 uptake capacity of the floodplain ecosystem. In addition, wet floodplain ecosystems with a large amount of peat accumulating annually in the soil will change to dry ecosystems with a large amount of carbon stored in aboveground standing biomass upon drainage (Shaver and Jonasson, 2001).

4.3 Soil temperature and TD effects on R_h

WTD and soil moisture content were lower in the drained transect, and this led to high diurnal fluctuations in soil temperatures at the shallow layers but colder soil temperatures at deeper layers with shallower TD compared to the undrained transect. Modifications in surface soil temperatures had greater impacts on CO_2 fluxes than in deep soil temperatures because surface soil is the place where decomposition rates are the largest because surface soils are more aerobic, contain larger amounts of highly labile organic matter, and are exposed to warmer soil temperatures. These factors were further affected by drainage.

Initially, a decrease in WTD due to drainage changes the soil to an aerobic condition especially at shallow layers. Anaerobic respiration is slower and less efficient than aerobic respiration, thus carbon release from both organic and mineral soils (surface and deep soil layers) under aerobic conditions can be 4 – 10 times higher than in anaerobic conditions (Lee et al., 2012). Thus changes from anaerobic to aerobic conditions due to drainage can dramatically increase decomposition rate.

Secondly, drained areas showed similar soil quality but a greater amount of organic carbon at the surface layers. The carbon to nitrogen (C:N) ratio is one of the critical factors that determine decomposability (Schädel et

Biogeosciences Discuss., doi:10.5194/bg-2015-629, 2016
Manuscript under review for journal Biogeosciences
Published: 18 January 2016

al., 2014). Although the litter decay rate is negatively correlated with the C:N ratio in the early stage of degradation (Enriquez et al., 1993), the soil C:N ratio decreases over time as organic matter loses C during
475 decomposition (Malmer and Holm, 1984), and more degraded organic matter with low C:N ratio can hardly be decomposed further (Schädel et al., 2014). Drainage did not alter C:N ratios of the surface peat layers but increased total carbon (%) by 11 % as well as bulk density by 44 % (data not shown), implying a larger amount of carbon is susceptible to decomposition at surface layers. On the other hand, when the proportion of shrub litter increase over a longer timescale, reduction in the quantity and quality of litter (Hobbie, 2008) will compensate
480 the elevated decomposition rate.

Lastly, drainage increases the soil surface temperature but lowers the deep soil temperatures, and this can possibly lead to a 93 % increase in R_h when these two opposing effects were combined. This increase is largely due to a greater amount of organic carbon – higher total carbon content as well as more compacted soil – in low-WTD sites affected by warmer temperatures at surface layers. Even though drainage has reduced soil
485 temperatures at deep layers and TD, the effects of the surface layers were larger, enhancing decomposition of organic matter and ER rates.

When all three factors are considered, the difference between the high- and the low-WTD sites were significant as we observed in the Figure 9. Magnitude of this ER increase ranged 7 – 27 % in 2013 and 9 – 63 % in 2014. This difference includes R_a so that the increases in R_h rates may become even higher when assuming the
490 ratio of total photosynthetic uptake to R_a is constant (Chapin et al., 2012a). However, effects of litter quality and quantity as well as contrasting influence of physical structures of vegetation on soil temperatures – negative relationship between shrub abundance and TD due to shade (Blok et al., 2010) and positive relationship due to decreased albedo (Bonfils et al., 2012) – need to be monitored in a longer term to gain further insight into, how all these factors together affect carbon accumulation and CO_2 fluxes.

Biogeosciences Discuss., doi:10.5194/bg-2015-629, 2016
Manuscript under review for journal Biogeosciences
Published: 18 January 2016

4.4 Frozen-season CO_2 flux

CO_2 fluxes in the frozen season were partially affected by vegetation group and soil temperatures but not in the same way as in the growing season. High and sporadic CO_2 fluxes in the drained transect can be partly explained by vegetation, soil temperatures and air pressure: high fluxes occurred when soil temperatures were relatively high and air pressure was decreasing in the presence of *Eriophorum* (Appendix 4). This may be a part of the physical processes suggested by Mastepanov et al. (2008, 2013), through which the freezing of soil pushes stored CO_2 and CH_4 gases in soil to the atmosphere through cracks in soil or dead plant bodies. Although soil temperatures until 35 cm were below zero, soil temperatures at 35 cm did not fall below -5 °C until the end of November. Ongoing freezing of soil with the combination of low air pressure could have stimulated CO_2 emission from soil to the atmosphere through dead *Eriophorum*. Another possibility is CO_2 production during the frozen season with relatively mild soil temperatures in early winter (Zimov et al., 1996). However, we cannot draw a firm conclusion that the observed sporadic high CO_2 fluxes in November were solely driven by these factors because we did not observe CO_2 fluxes continuously with soil temperatures, and these high CO_2 fluxes were only observed in the drained transect in spite of similar conditions in the two transects. High uncertainties and limitations to predict the frozen season CO_2 fluxes in addition to possible high CO_2 fluxes during the thawing season (Friborg et al., 1997) should be overcome to estimate the annual CO_2 fluxes of this site. Nevertheless, considerably higher CO_2 fluxes in the frozen season in the drained transect implies that drainage not only affects the growing-season CO_2 fluxes but also non-growing-season fluxes significantly.

5 Conclusion and final remarks

Drainage of the Chersky site resulting in a drop in WTD by 20 cm substantially altered ecosystem properties both biogeophysically and biogeochemically over the span of a decade, resulting in important present-

Biogeosciences Discuss., doi:10.5194/bg-2015-629, 2016
Manuscript under review for journal Biogeosciences
Published: 18 January 2016

day differences in CO_2 fluxes. Firstly, vegetation community structure in drained sites was significantly shifted toward more *Carex* species and shrub species (*Betula* and *Salix* species) but less *Eriophorum*. Secondly, WTD variation endowed divergent soil temperature regimes by depth: low-WTD sites showed stronger fluctuations in soil surface temperatures due to low heat capacity and colder deep soil temperatures due to low thermal conductivity of dry soils. Consequently the low-WTD sites had thinner thaw depths.

These aboveground and belowground changes significantly affected CO_2 fluxes. Dominant plant species in the low-WTD sites – *Carex* species – took up less amount of CO_2 (lower GPP) than *Eriophorum* which is dominant in the high-WTD sites. Increased abundance of shrubs did not affect GPP significantly but this could be from underestimated shrub species of the observation sites. The low-WTD sites showed higher ER due to more aerobic condition with a greater amount of organic carbon affected by higher soil surface temperatures. Overall, drainage increased net CO_2 uptake (NEE) by 16 % in 2013 but decreased it by 37 % during the 2014 growing season. Although these results are influenced by climatic inter-annual variability, drainage overall tended to reduce net CO_2 uptake during the growing season. In addition frozen season CO_2 emission was four times larger in the drained than undrained transect partially due to modifications in dominant vegetation species and soil temperatures.

In conclusion, a decade-long drainage in the Chersky ecosystem significantly affected carbon cycle processes with a decrease in the net CO_2 uptake during the growing season and an increase in the net CO_2 emission during the frozen season. The observed decreases in net C uptake following a decade of drainage may be prolonged in the future (Zona et al., 2010).

Acknowledgements

Biogeosciences Discuss., doi:10.5194/bg-2015-629, 2016
Manuscript under review for journal Biogeosciences
Published: 18 January 2016

This work has been supported by the European Commission (PAGE21 project, FP7-ENV-2011, Grant Agreement No. 282700, and PerCCOM project, FP7-PEOPLE-2012-CIG, Grant Agreement No. PCIG12-GA-2012-333796), the German Ministry of Education and Research (CarboPerm-Project, BMBF Grant No. 03G0836G), and the AXA Research Fund (PDOC_2012_W2 campaign, ARF fellowship M.Goeckede). Authors appreciate NESS staffs especially Galina Zimova, Nastya Zimova and Vladimir Tatayev for organizing and assisting field works; Chiara Corradi and Lutz Merbold for giving us valuable advice; Olaf Kolle, Martin Hertel, Frank Voigt, Waldemar Ziegler and other Freiland group members for technical support; Ina Burjack, Marcus Wildner, Carsten Schaller and Fanny Kittler for assisting field work; Mirco Migliavacca for advising data analysis; Ines Hilke and other RoMA group members for soil analysis.

We applied first-last-author-emphasis and equal-contribution (alphabetical sequence) methods for the order of authors (Tscharntke et al., 2007).

Biogeosciences Discuss., doi:10.5194/bg-2015-629, 2016
Manuscript under review for journal Biogeosciences
Published: 18 January 2016

References

Billings, W. D., Luken, J. O., Mortensen, D. A. and Peterson, K. M.: Arctic tundra a source or sink for atmospheric carbon dioxide in a changing environmnet?, Oecologia (Berlin), 53(1), 7–11, 1982.

Bintanja, R. and Selten, F. M.: Future increases in Arctic precipitation linked to local evaporation and sea-ice retreat., Nature, 509(7501), 479–482, doi:10.1038/nature13259, 2014.

Blok, D., Heijmans, M. M. P. D., Schaepman-Strub, G., Kononov, A. V., Maximov, T. C. and Berendse, F.: Shrub expansion may reduce summer permafrost thaw in Siberian tundra, Glob. Chang. Biol., 16(4), 1296–1305, doi:10.1111/j.1365-2486.2009.02110.x, 2010.

Bond-Lamberty, B. and Thomson, A.: Temperature-associated increases in the global soil respiration record., Nature, 464(7288), 579–82, doi:10.1038/nature08930, 2010.

Bonfils, C. J. W., Phillips, T. J., Lawrence, D. M., Cameron-Smith, P., Riley, W. J. and Subin, Z. M.: On the influence of shrub height and expansion on northern high latitude climate, Environ. Res. Lett., 7(1), 015503, doi:10.1088/1748-9326/7/1/015503, 2012.

Chapin, F. S., Matson, P. A. and Vitousek, P. M.: Carbon inputs to ecosystems, in Principles of terrestrial ecosystem ecology, pp. 123–156, Springer New York., 2012a.

Chapin, F. S., Matson, P. A. and Vitousek, P. M.: Plant carbon budgets, in Principles of terrestrial ecosystem ecology, pp. 157–182, Springer New York., 2012b.

Christensen, T. R., Friborg, T., Sommerkorn, M., Kaplan, J., Illeris, L., Soegaard, H., Nordstroem, C. and Jonasson, S.: Trace gas exchange in a high-Arctic valley: 1. Variationsin CO2 and CH4 flux between tundra vegetation types, Global Biogeochem. Cycles, 14(3), 701–713, doi:10.1029/1999GB001134, 2000.

Collins, M., Knutti, R., Arblaster, J., Dufresne, J.-L., Fichefet, T., Friedlingstein, P., Gao, X., Gutowski, W. J., Johns, T., Krinner, G., Shongwe, M., Tebaldi, C., Weaver, A. J. and Wehne, M.: Long-term Climate Change: Projections, Commitments and Irreversibility, in Climate Change 2013: The Physical Science Basis. Contribution of Working Group I to the Fifth Assessment Report of the Intergovernmental Panel on Climate Change, Cambridge University Press, Cambridge and New York., 2013.

Corradi, C., Kolle, O., Walter, K., Zimov, S. A. and Schulze, E. D.: Carbon dioxide and methane exchange of a north-east Siberian tussock tundra, Glob. Chang. Biol., 11(11), 1910–1925, doi:10.1111/j.1365-2486.2005.01023.x, 2005.

Curtis, J., Wendler, G., Stone, R. and Dutton, E.: Precipitation decrease in the western Arctic, with special emphasis on Barrow and Barter Island, Alaska, Int. J. Climatol., 18(15), 1687–1707, doi:10.1002/(SICI)1097-0088(199812)18:15<1687::AID-JOC341>3.0.CO;2-2, 1998.

Enriquez, S., Duarte, C. M. and Sand-Jensen, K.: Patterns in decomposition rates among photosynthetic organisms: the importance of detritus C:N:P content, Oecologia (Germany) [online] Available from: http://agris.fao.org/agris-search/search.do?recordID=DE93K0839 (Accessed 17 November 2015), 1993.

Epstein, H. E., Raynolds, M. K., Walker, D. A., Bhatt, U. S., Tucker, C. J. and Pinzon, J. E.: Dynamics of aboveground phytomass of the circumpolar Arctic tundra during the past three decades, Environ. Res. Lett., 7(1), 015506, doi:10.1088/1748-9326/7/1/015506, 2012.

Friborg, T., Christensen, T. R. and Søgaard, H.: Rapid response of greenhouse gas emission to early spring thaw in a subarctic mire as shown by micrometeorological techniques, Geophys. Res. Lett., 24(23), 3061–3064, doi:10.1029/97GL03024, 1997.

Hobbie, S. E.: Temperature and plant species control over litter decomposition in Alaskan tundra, Ecol. Monogr., 66(4), 503–522, doi:10.2307/2963492, 2008.

Huemmrich, K. F., Kinoshita, G., Gamon, J. A., Houston, S., Kwon, H. and Oechel, W. C.: Tundra carbon balance under varying temperature and moisture regimes, J. Geophys. Res., 115, doi:10.1029/2009jg001237, 2010.

Hugelius, G., Strauss, J., Zubrzycki, S., Harden, J. W., Schuur, E. A. G., Ping, C.-L., Schirrmeister, L., Grosse, G., Michaelson, G. J., Koven, C. D., O'Donnell, J. A., Elberling, B., Mishra, U., Camill, P., Yu, Z., Palmtag, J. and Kuhry, P.: Estimated stocks of circumpolar permafrost carbon with quantified uncertainty ranges and identified data gaps, Biogeosciences, 11(23), 6573–6593, doi:10.5194/bg-11-6573-2014, 2014.

Huntington, T. G.: Evidence for intensification of the global water cycle: Review and synthesis, J. Hydrol., 319(1-4), 83–95, doi:10.1016/j.jhydrol.2005.07.003, 2006.

Jia, G. J.: Greening of arctic Alaska, 1981–2001, Geophys. Res. Lett., 30(20), 2067, doi:10.1029/2003GL018268, 2003.

Johnson, L. C., Shaver, G. R., Giblin, A. E., Nadelhoffer, K. J., Rastetter, E. R., Laundre, J. A. and Murray, G. L.: Effects of drainage and temperature on carbon balance of tussock tundra microcosms, Oecologia, 108(4), 737–748, doi:10.1007/bf00329050, 1996.

Jorgenson, M. T., Shur, Y. L. and Pullman, E. R.: Abrupt increase in permafrost degradation in Arctic Alaska, Geophys. Res. Lett., 33(2), L02503, doi:10.1029/2005GL024960, 2006.

Kattsov, V. M. and Walsh, J. E.: Twentieth-century trends of Arctic precipitation from observational data and a climate model simulation, J. Clim., 13(8), 1362–1370, doi:10.1175/1520-0442(2000)013<1362:TCTOAP>2.0.CO;2, 2000.

Kim, Y.: Effect of thaw depth on fluxes of CO2 and CH4 in manipulated Arctic coastal tundra of Barrow, Alaska., Sci. Total Environ., 505, 385–389, doi:10.1016/j.scitotenv.2014.09.046, 2015.

Kirtman, B., Power, S. B., Adedoyin, J. A., Boer, G. J., Bojariu, R., Camilloni, I., Doblas-Reyes, F. J., Fiore, A. M., Kimoto, M., Meehl, G. A., Prather, M., Sarr, A., Schär, C., Sutton, R., Oldenborgh, G. J. van, Vecchi, G. and Wan, H. J.: Near-term Climate Change: Projections and Predictability, in Climate Change 2013: The Physical Science Basis. Contribution of Working Group I to the Fifth Assessment Report of the Intergovernmental Panel on Climate Change, Cambridge University Press, Cambridge and New York., 2013.

Koven, C. D., Ringeval, B., Friedlingstein, P., Ciais, P., Cadule, P., Khvorostyanov, D., Krinner, G. and Tarnocai, C.: Permafrost carbon-climate feedbacks accelerate global warming, Proc. Natl. Acad. Sci. U. S. A., 108(36), 14769–74, doi:10.1073/pnas.1103910108, 2011.

Lee, H., Schuur, E. A. G., Inglett, K. S., Lavoie, M. and Chanton, J. P.: The rate of permafrost carbon release under aerobic and anaerobic conditions and its potential effects on climate, Glob. Chang. Biol., 18(2), 515–527, doi:10.1111/j.1365-2486.2011.02519.x, 2012.

Luus, K. A. and Lin, J. C.: The Polar Vegetation Photosynthesis and Respiration Model: a parsimonious, satellite-data-driven model of high-latitude CO2 exchange, Geosci. Model Dev., 8, 2655–2674, doi:10.5194/gmd-

8-2655-2015, 2015.

Malmer, N. and Holm, E.: Variation in the C/N-quotient of peat in relation to decomposition rate and age determination with 210Pb, Oikos, 43, 171–182, 1984.

Mastepanov, M., Sigsgaard, C., Tagesson, T., Ström, L., Tamstorf, M. P., Lund, M. and Christensen, T. R.: Revisiting factors controlling methane emissions from high-Arctic tundra, Biogeosciences, 10(7), 5139–5158, doi:10.5194/bg-10-5139-2013, 2013.

McEwing, K. R., Fisher, J. P. and Zona, D.: Environmental and vegetation controls on the spatial variability of CH4 emission from wet-sedge and tussock tundra ecosystems in the Arctic., Plant Soil, 388(1-2), 37–52, doi:10.1007/s11104-014-2377-1, 2015.

Merbold, L., Kutsch, W. L., Corradi, C., Kolle, O., Rebmann, C., Stoy, P. C., Zimov, S. A. and Schulze, E. D.: Artificial drainage and associated carbon fluxes (CO2/CH4) in a tundra ecosystem, Glob. Chang. Biol., 15(11), 2599–2614, doi:10.1111/j.1365-2486.2009.01962.x, 2009.

Myneni, R. B., Keeling, C. D., Tucker, C. J., Asrar, G. and Nemani, R. R.: Increased plant growth in the northern high latitudes from 1981 to 1991, Nature, 386(6626), 698–702, doi:10.1038/386698a0, 1997.

Natali, S., Schuur, T., Mauritz, M., Schade, J., Celis, G., Crummer, G., Johnston, C., Krapek, J., Pegoraro, E., Salmon, V. and Webb, E.: Permafrost thaw and soil moisture drive CO2 and CH4 release from upland tundra, J. Geophys. Res. Biogeosciences, 120(3), 525–537, doi:10.1002/2014JG002872, 2015.

O'Donnell, J. A., Jorgenson, M. T., Harden, J. W., McGuire, A. D., Kanevskiy, M. Z. and Wickland, K. P.: The effects of permafrost thaw on soil hydrologic, thermal, and carbon dynamics in an Alaskan peatland, Ecosystems, 15(2), 213–229, doi:10.1007/s10021-011-9504-0, 2011.

Oechel, W. C., Vourlitis, G. L., Hastings, S. J., Ault, R. P. and Bryant, P.: The effects of water table manipulation and elevated temperature on the net CO2 flux of wet sedge tundra ecosystems, Glob. Chang. Biol., 4(1), 77–90, doi:10.1046/j.1365-2486.1998.00110.x, 1998.

Oechel, W. C., Vourlitis, G. L., Hastings, S. J., Zulueta, R. C., Hinzman, L. and Kane, D.: Acclimation of ecosystem CO2 exchange in the Alaskan Arctic in response to decadal climate warming, Nature, 406(6799), 978–981, doi:10.1038/35023137, 2000.

Olivas, P. C., Oberbauer, S. F., Tweedie, C. E., Oechel, W. C. and Kuchy, A.: Responses of CO2 flux components of Alaskan Coastal Plain tundra to shifts in water table, J. Geophys. Res., 115, doi:10.1029/2009jg001254, 2010.

Overland, J. E., Wang, M., Walsh, J. E. and Stroeve, J. C.: Future Arctic climate changes: Adaptation and mitigation time scales, Earth's Futur., 2(2), 68–74, doi:10.1002/2013EF000162, 2014.

Peterson, K. M., Billings, W. D. and Reynolds, D. N.: Influence of water-table and atmospheric CO2 concentration on the carbon balance of Arctic tundra , Arct. Alp. Res., 16(3), 331–335, doi:10.2307/1550942, 1984.

R Core Team: R: A language and environment for statistical computing, [online] Available from: http://www.r-project.org, 2013.

Reliable Prognosis: http://www.rp5.ru, last access: 2 Nov, 2015

Saugier, B., Roy, J. and Mooney, H. A.: Estimations of global terrestrial productivity: converging toward a single number?, in Terrestrial Global Productivity, pp. 543–557, Elsevier., 2001.

Schädel, C., Schuur, E. A. G., Bracho, R., Elberling, B., Knoblauch, C., Lee, H., Luo, Y., Shaver, G. R. and Turetsky, M. R.: Circumpolar assessment of permafrost C quality and its vulnerability over time using long-term incubation data., Glob. Chang. Biol., 20(2), 641–52, doi:10.1111/gcb.12417, 2014.

Schaefer, K., Zhang, T., Bruhwiler, L. and Barrett, A. P.: Amount and timing of permafrost carbon release in response to climate warming, Tellus B, 63(2), 165–180, doi:10.1111/j.1600-0889.2011.00527.x, 2011.

Schaefer, K., Lantuit, H., Romanovsky, V. E., Schuur, E. A. G. and Witt, R.: The impact of the permafrost carbon feedback on global climate, Environ. Res. Lett., 9(8), 085003, doi:10.1088/1748-9326/9/8/085003, 2014.

Schuur, E. A. G., McGuire, A. D., Schädel, C., Grosse, G., Harden, J. W., Hayes, D. J., Hugelius, G., Koven, C. D., Kuhry, P., Lawrence, D. M., Natali, S. M., Olefeldt, D., Romanovsky, V. E., Schaefer, K., Turetsky, M. R., Treat, C. C. and Vonk, J. E.: Climate change and the permafrost carbon feedback, Nature, 520(7546), 171–179, doi:10.1038/nature14338, 2015.

Serreze, M. C., Walsh, J. E., III, F. S. C., Osterkamp, T., Dyurgerov, M., Romanovsky, V., Oechel, W. C., Morison, J., Zhang, T. and Barry, R. G.: Observational evidence of recent change in the northern high-latitude environment, Clim. Change, 46(1-2), 159–207, doi:10.1023/A:1005504031923, 2000.

Shaver, G. R. and Jonasson, S.: Productivity of Arctic ecosystems, in Terrestrial Global Productivity, pp. 189–210, Elsevier., 2001.

Stafford, J. M., Wendler, G. and Curtis, J.: Temperature and precipitation of Alaska: 50 year trend analysis, Theor. Appl. Climatol., 67(1-2), 33–44, doi:10.1007/s007040070014, 2000.

Tarnocai, C., Canadell, J. G., Schuur, E. A. G., Kuhry, P., Mazhitova, G. and Zimov, S.: Soil organic carbon pools in the northern circumpolar permafrost region, Glob. Biogeochem. Cycles, 23(2), GB2023, doi:10.1029/2008GB003327, 2009.

Tscharntke, T., Hochberg, M. E., Rand, T. A., Resh, V. H. and Krauss, J.: Author sequence and credit for contributions in multiauthored publications, PLoS Biol., 5(1), e18, doi:10.1371/journal.pbio.0050018, 2007.

Xu, L., Myneni, R. B., Chapin III, F. S., Callaghan, T. V., Pinzon, J. E., Tucker, C. J., Zhu, Z., Bi, J., Ciais, P., Tømmervik, H., Euskirchen, E. S., Forbes, B. C., Piao, S. L., Anderson, B. T., Ganguly, S., Nemani, R. R., Goetz, S. J., Beck, P. S. A., Bunn, A. G., Cao, C. and Stroeve, J. C.: Temperature and vegetation seasonality diminishment over northern lands, Nat. Clim. Chang., 3(6), 581–586, doi:10.1038/nclimate1836, 2013.

Zhou, T., Shi, P., Hui, D. and Luo, Y.: Global pattern of temperature sensitivity of soil heterotrophic respiration (Q 10) and its implications for carbon-climate feedback, J. Geophys. Res., 114(G2), G02016, doi:10.1029/2008JG000850, 2009.

Zimov, S. A., Davidov, S. P., Voropaev, Y. V., Prosiannikov, S. F., Semiletov, I. P., Chapin, M. C. and Chapin, F. S.: Siberian CO2 efflux in winter as a CO2 source and cause of seasonality in atmospheric CO2, Clim. Change, 33(1), 111–120, doi:10.1007/BF00140516, 1996.

Zona, D., Oechel, W. C., Peterson, K. M., Clements, R. J., U, K. T. P. and Ustin, S. L.: Characterization of the carbon fluxes of a vegetated drained lake basin chronosequence on the Alaskan Arctic Coastal Plain, Glob. Chang. Biol., 16(6), 1870–1882, doi:10.1111/j.1365-2486.2009.02107.x, 2010.

700 Zona, D., Lipson, D. A., Zulueta, R. C., Oberbauer, S. F. and Oechel, W. C.: Microtopographic controls on ecosystem functioning in the Arctic Coastal Plain, J. Geophys. Res., 116, G00I08, doi:10.1029/2009JG001241, 2011.

Biogeosciences Discuss., doi:10.5194/bg-2015-629, 2016
Manuscript under review for journal Biogeosciences
Published: 18 January 2016

Table 1 CO_2 flux changes (mole-CO_2 m^{-2} day^{-1}) in response to a water table depth (WTD) decrease (cm), expressed as either $flux_{control} - flux_{lower\text{-}WTD}$ or $flux_{higher\text{-}WTD} - flux_{lower\text{-}WTD}$. Negative net CO_2 flux rates represent a net increase in terrestrial CO_2 uptake, thus positive changes denote a decrease in net CO_2 uptake by terrestrial ecosystem or an increase in terrestrial CO_2 emissions to the atmosphere. The ranges of these changes are from different years, soil types, and study sites. Numbers in parentheses represent percent change compared to the original (control, WTD condition) flux.

Sites	WTD change	Net CO_2 flux change	Reference
Coastal plain	Drawdown	+ 0.05 (+160 %)	Huemmrich et al. (2010)
	3 cm lower	+ 0.02 (+87 %)	Olivas et al. (2010) [1]
	Up to 3.6 cm lower *	+ 0.10 (+63 %)	Christensen et al. (2000) [2]
	7- 7.5cm lower	+ 0.03 (+450 %)	Oechel et al. (1998)
	8.5 cm lower	+ 0.25 (+365 %)	Kim (2015) [3]
	11.9 cm lower *	+ 0.03 (+67 %)	Zona et al. (2011) [3]
	20 cm lower *	+ 0.06 (+37 %)	McEwing et al. (2015)
Floodplain	20-35 cm lower	- 0.005 (-47 %)	Merbold et al. (2009) [4]
Moist tundra	2.5 cm lower	- 0.002 (-3 %)	Natali et al. (2015) [5]
Laboratory	Saturated	- 0.22 to - 0.12	Johnson et al. (1996)

Biogeosciences Discuss., doi:10.5194/bg-2015-629, 2016
Manuscript under review for journal Biogeosciences
Published: 18 January 2016

vs. field capacity	(-1716 to -344 %)	
5 cm lower	- 0.05 to + 0.08	Billings et al. (1982)
	(-59 to +72 %)	
10 cm lower	+ 0.18 (+184 %)	Peterson et al. (1984)

* WTD difference from natural variation instead of manipulation

[1] Only the data of the year 2008 were used when the WTD of drained site was lower than that of control

[2] Only from grassland data

[3] Only ecosystem respiration was considered (no gross primary production)

[4] Only the data of the year 2003 and 2005 were used when the climate conditions were similar

[5] Only the data of the year 2013 were used when the WTD of drained site was lower than that of control

Biogeosciences Discuss., doi:10.5194/bg-2015-629, 2016
Manuscript under review for journal Biogeosciences
Published: 18 January 2016

Table 2 Characteristics of vegetation and water table depth (WTD) of observation sites. Vegetation groups were created when the relative abundance of each species exceeded 10 %. Average WTD (cm) was calculated by pooling all WTD measured in both years by each vegetation group, except the period where the whole area was flooded from snowmelt (mean ± standard deviation). When the average WTD of the growing season was larger than -10 cm, sites were classified as high-WTD group.

Transect	Observation sites	Vegetation group	Average WTD	WTD group
Drained	0	EriophorumShrub	4.6 ± 2.2	High
	1, 2, 4	CarexEriophorum	-14.1 ± 8.4	Low
	3, 5, 6, 7, 8, 9	Carex	-19.2 ± 6.1	Low
Undrained	0	CarexShrub	-1.3 ± 2.3	High
	1, 3, 6, 7, 8, 9	Eriophorum	4.3 ± 2.4	High
	2	EriophorumShrub	3.9 ± 2.1	High
	4, 5	CarexShrub	-18.5 ± 4.1	Low

Biogeosciences Discuss., doi:10.5194/bg-2015-629, 2016
Manuscript under review for journal Biogeosciences
Published: 18 January 2016

Table 3 Two-way ANCOVA results with water table depth (WTD) category (high and low) and depth (cm) as independent variables and soil temperatures (°C) as dependent variable. Periods of 2013 and three sub-seasons of 2014 were separately analyzed. *F* and *P* values are presented in numbers and asterisks (*P* value < 0.001 ***, < 0.01 **, < 0.05 *).

	Transect	WTD	Depth	WTD*Depth
2013	Drained	12.75 ***	602.64 ***	13.38 ***
	Undrained	15.38 ***	700.93 ***	2.64
2014.1	Drained	3.54	169.46 ***	0.02
	Undrained	32.55 ***	165.35 ***	29.56 ***
2014.2	Drained	26.21 ***	400.48 ***	0.52
	Undrained	1.24	380.91 ***	2.42
2014.3	Drained	101.87 ***	680.50 ***	7.55 **
	Undrained	6.49 *	813.62 ***	4.91 *

Biogeosciences Discuss., doi:10.5194/bg-2015-629, 2016
Manuscript under review for journal Biogeosciences
Published: 18 January 2016

Table 4 Root mean squared error (RMSE) and mean bias error (MBE) of the observed and the extrapolated fluxes (μmole-CO_2 m^{-2} s^{-1}). The observed fluxes indicate those used for calibration.

Year	Group	Ecosystem respiration		Gross primary production	
		RMSE	MBE	RMSE	MBE
2013	D_Carex	0.7	0.003	2.1	-2.9
	D_CarexEriophorum	0.6	-0.130	1.0	-0.1
	D_Eriophorumshrub	0.8	0.004	2.2	-2.4
	U_CarexShrub	0.7	0.002	1.3	-2.9
	U_Eriophorum	0.5	-0.001	1.4	-2.3
	U_EriophorumShrub	0.5	0.0002	1.2	-2.8
2014	D_high (EriophorumShrub)	0.5	-0.003	2.5	-4.5
	D_low (CarexEriophorum)	0.7	-0.005	1.9	-4.5
	U_high (EriophorumShrub)	0.9	-0.002	1.9	-3.6
	U_low (CarexShrub)	0.9	0.015	2.5	-7.6

730

Biogeosciences Discuss., doi:10.5194/bg-2015-629, 2016
Manuscript under review for journal Biogeosciences
Published: 18 January 2016

Table 5 Cumulative flux (mole-CO_2 m^{-2}) from extrapolation. Results of 2013 are from fits of all data points ± standard deviation from bootstrapping, and those of 2014 of mean ± standard deviation from bootstrapping. Net ecosystem exchange (NEE) was calculated by subtracting gross primary production (GPP) from ecosystem respiration (ER), indicating positive values are CO_2 emission to the atmosphere, and negative values are CO_2 uptake by terrestrial ecosystem. Period of 2013: 22 July to 10 August (20 days), 2014: 16 June to 20 August (66 days).

Year	Group	ER	GPP	NEE
2013	D_Carex	3.4 ± 0.2	5.7 ± 0.0	-2.3 ± 0.2
	D_CarexEriophorum	3.1 ± 0.3	5.5 *	-2.3 ± 0.4
	D_EriophorumShrub	3.1 ± 0.9	8.0 *	-4.9 ± 0.6
	U_CarexShrub	3.4 ± 0.1	4.3 ± 0.0	-0.9 ± 0.1
	U_Eriophorum	2.9 ± 0.1	5.7 ± 0.0	-2.7 ± 0.1
	U_EriophorumShrub	3. 9 ± 0.3	5.5 ± 0.0	-1.6 ± 0.2
2014	D_high (EriophorumShrub)	15.3 ± 0. 8	33.7 ± 0.5	-18.4 ± 0.3
	D_low(CarexEriophorum)	16.6 ± 0.8	22.8 ± 0.3	-6.1 ± 0.5
	U_high (EriophorumShrub)	13.5 ± 1.2	26.0 ± 0.1	-12.5 ± 1.1
	U_low (CarexShrub)	18.5 ± 1.0	27.6 ± 0.1	-9.1 ± 0.8

* No error due to lack of bootstrapping results, thus error range of NEE is only from ER

Biogeosciences Discuss., doi:10.5194/bg-2015-629, 2016
Manuscript under review for journal Biogeosciences
Published: 18 January 2016

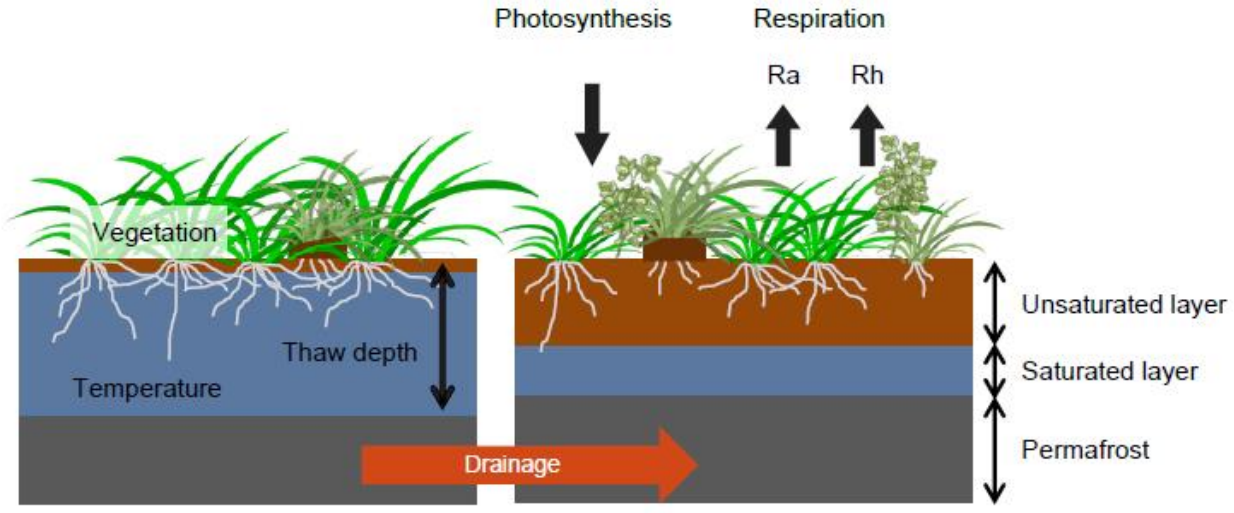

740 Figure 1 A schematic showing how drainage events affect a floodplain ecosystem and CO_2 fluxes: drainage of a floodplain ecosystem would replace wetland grasses by shrubs, alter soil temperatures and thaw depths, and these modifications will subsequently affect CO_2 fluxes by changing the rates of photosynthesis as well as autotrophic and heterotrophic respiration (R_a and R_h).

Biogeosciences Discuss., doi:10.5194/bg-2015-629, 2016
Manuscript under review for journal Biogeosciences
Published: 18 January 2016

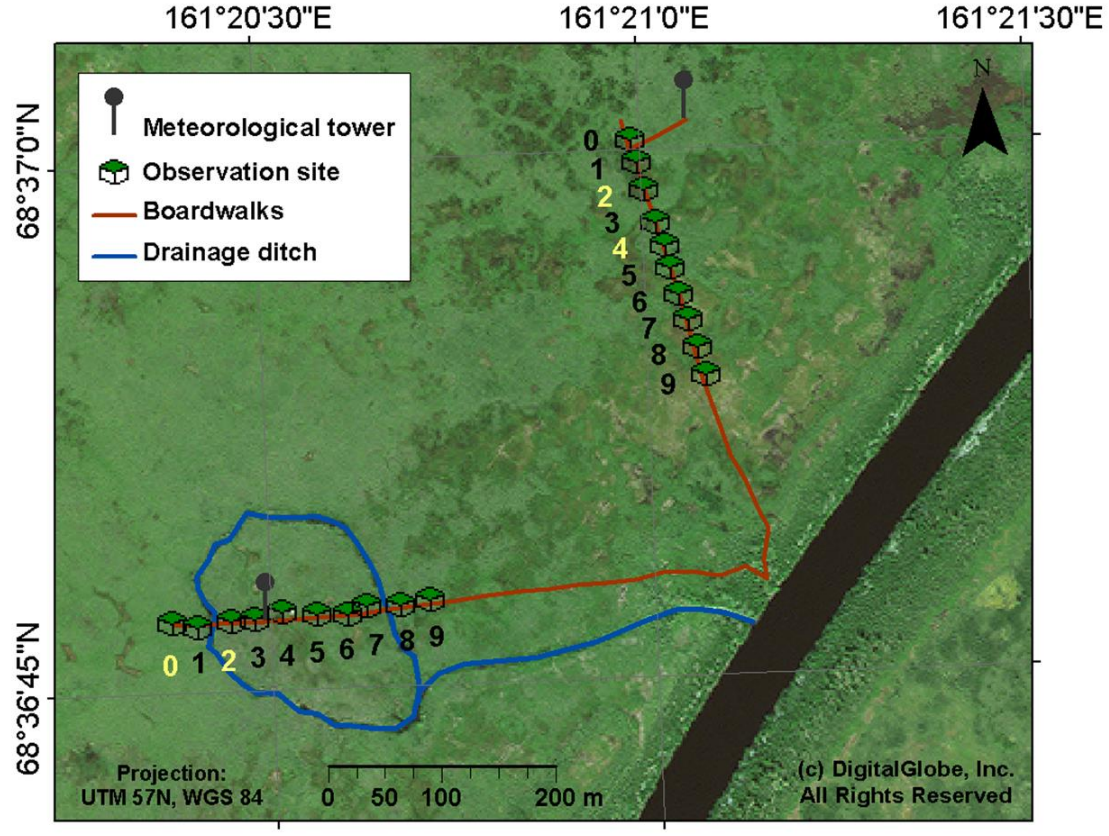

745 Figure 2 A schematic of a site setup with the drained (bottom left) and the undrained (top right) transects. Names of observation sites are written with numbers and two core sites in each transect are highlighted in yellow.

Biogeosciences Discuss., doi:10.5194/bg-2015-629, 2016
Manuscript under review for journal Biogeosciences
Published: 18 January 2016

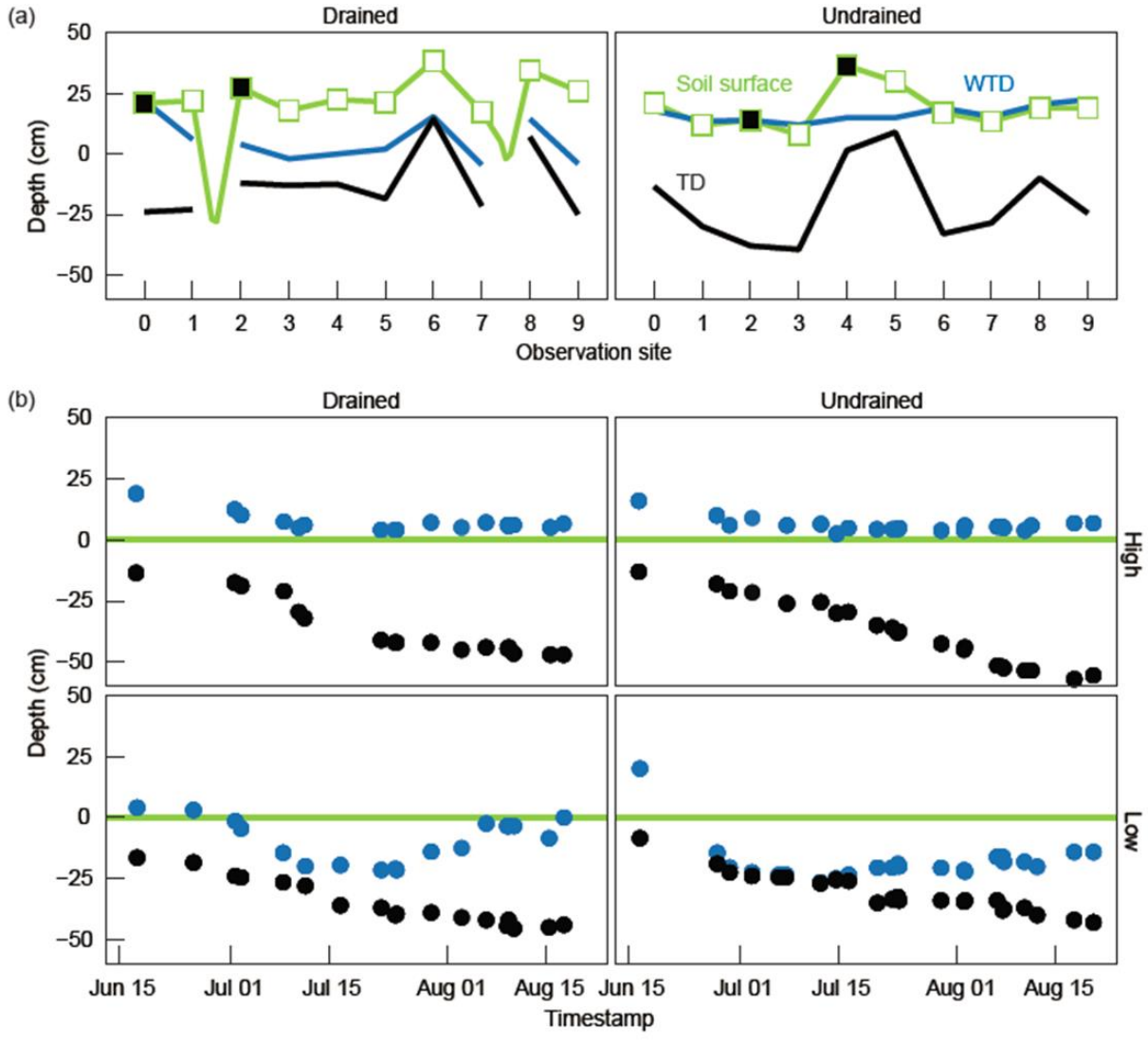

Figure 3 (a) Spatial variability in water table depths (WTD, blue lines) and thaw depths (TD, black lines) measured across the two transects on the August 10, 2013. The observation sites are indicated with open squares while the core sites with closed squares with relative terrain heights (green lines). (b) Temporal variability in

Biogeosciences Discuss., doi:10.5194/bg-2015-629, 2016
Manuscript under review for journal Biogeosciences
Published: 18 January 2016

WTD (blue points) and TD (black points) observed at the four core sites over the growing season of 2014, separated by transect (columns) and WTD category (rows). Green lines represent soil surface.

Biogeosciences Discuss., doi:10.5194/bg-2015-629, 2016
Manuscript under review for journal Biogeosciences
Published: 18 January 2016

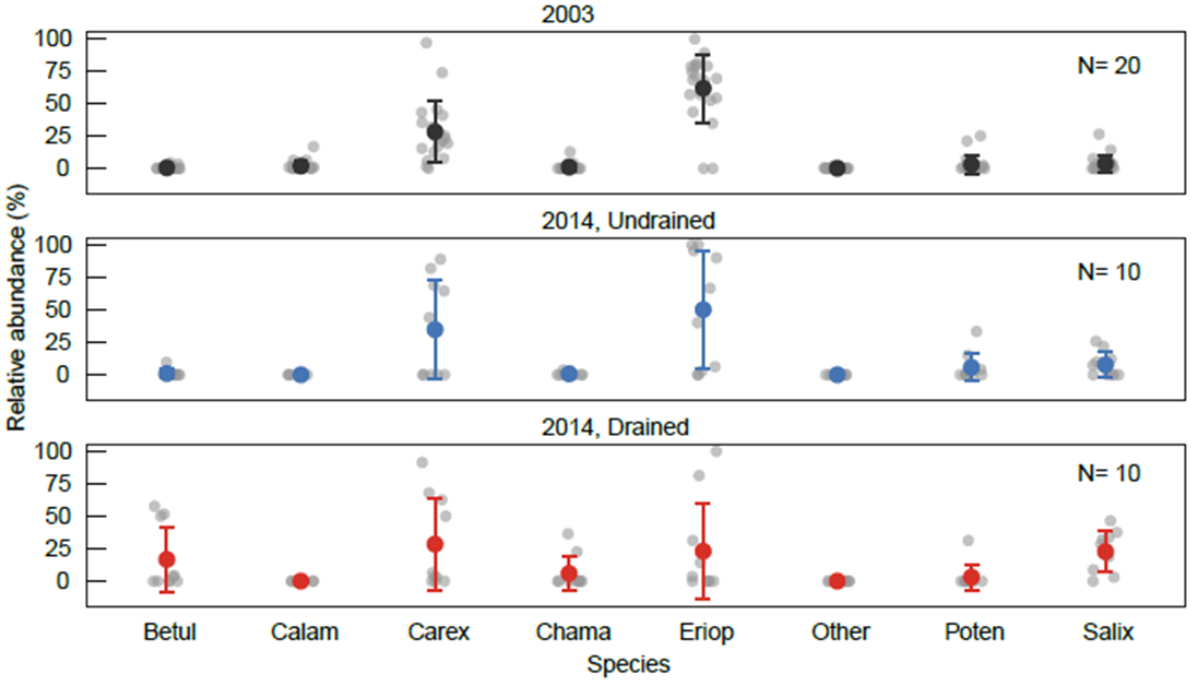

Figure 4 Abundances of vegetation species observed across the transects (small gray points) with large colored points and error bars showing the mean values and the standard deviations. Betul: *Betula Exilis*, Calam: *Calamagrostis purpurascens*, Carex: *Carex* species, Chama: *Chamaedaphne calyculata*, Eriop: *Eriophorum Angustifolium*, Poten: *Potentila Palustris*, Salix: *Salix species*.

Biogeosciences Discuss., doi:10.5194/bg-2015-629, 2016
Manuscript under review for journal Biogeosciences
Published: 18 January 2016

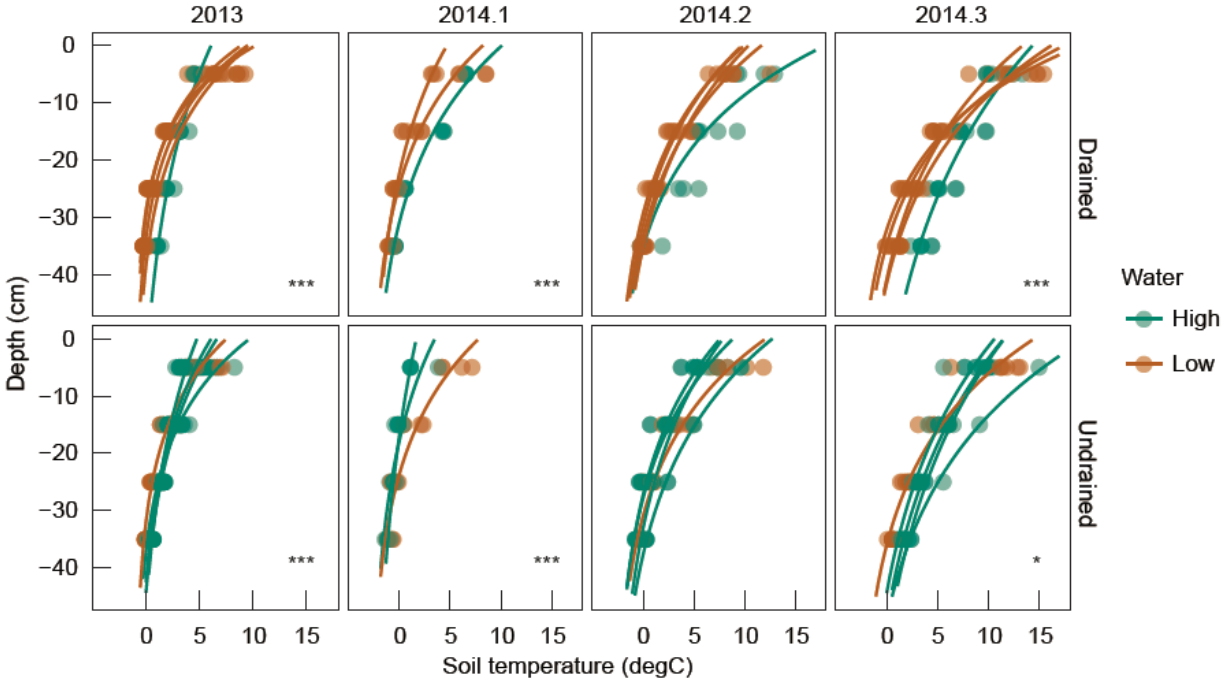

Figure 5 Soil temperature profiles based on observations at 5, 15, 25, and 35 cm depths (points: observed, lines: exponentially interpolated) from the 5 observation sites each at the drained (top) and the undrained (bottom) transects. To minimize the impacts of the diurnal temperature cycle on this temporally discontinuous dataset, the time window for averaging was restricted to 1 to 5 pm. Panels from left to right show data from 2013 and three sub-seasons of the growing season of 2014, respectively, where green color indicates sites with high water table depths (WTD) and brown indicates those with low WTD. Data subsets where significant differences in WTD between the high- and the low-WTD sites were detected are marked with asterisks (*P* value < 0.001 ***, < 0.01 **, < 0.05 *).

Biogeosciences Discuss., doi:10.5194/bg-2015-629, 2016
Manuscript under review for journal Biogeosciences
Published: 18 January 2016

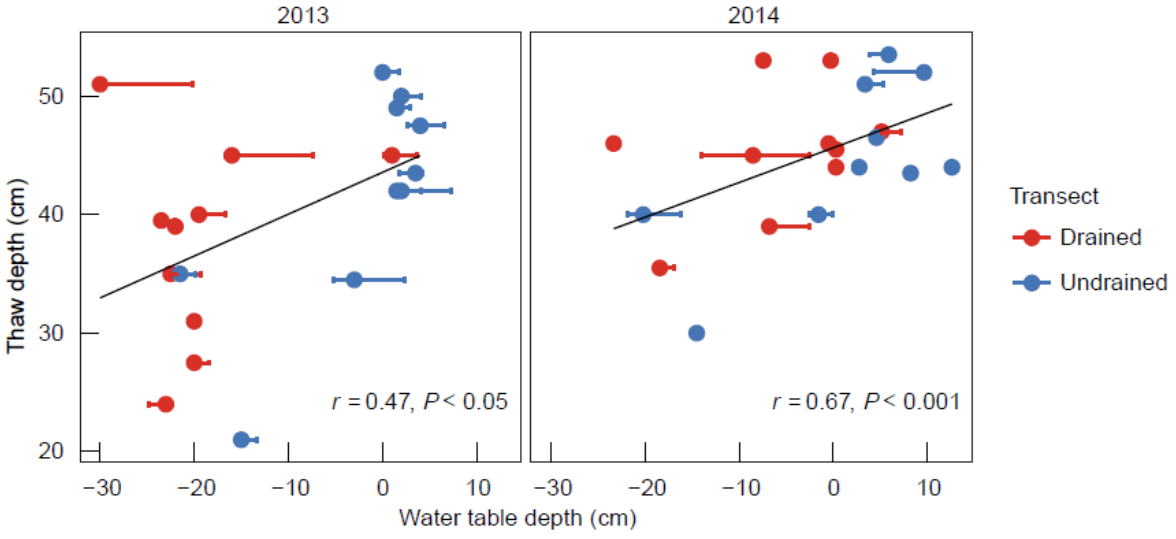

Figure 6 Correlations of thaw depths (TD) and water table depths (WTD) in the middle of August in 2013 and 2014, where red points indicate sites from the drained transect, blue points sites from the undrained transect. Error bars of WTD represent the minimum and the maximum ranges of WTD of the previous 20 days. Results of correlation analysis of each year are presented.

Biogeosciences Discuss., doi:10.5194/bg-2015-629, 2016
Manuscript under review for journal Biogeosciences
Published: 18 January 2016

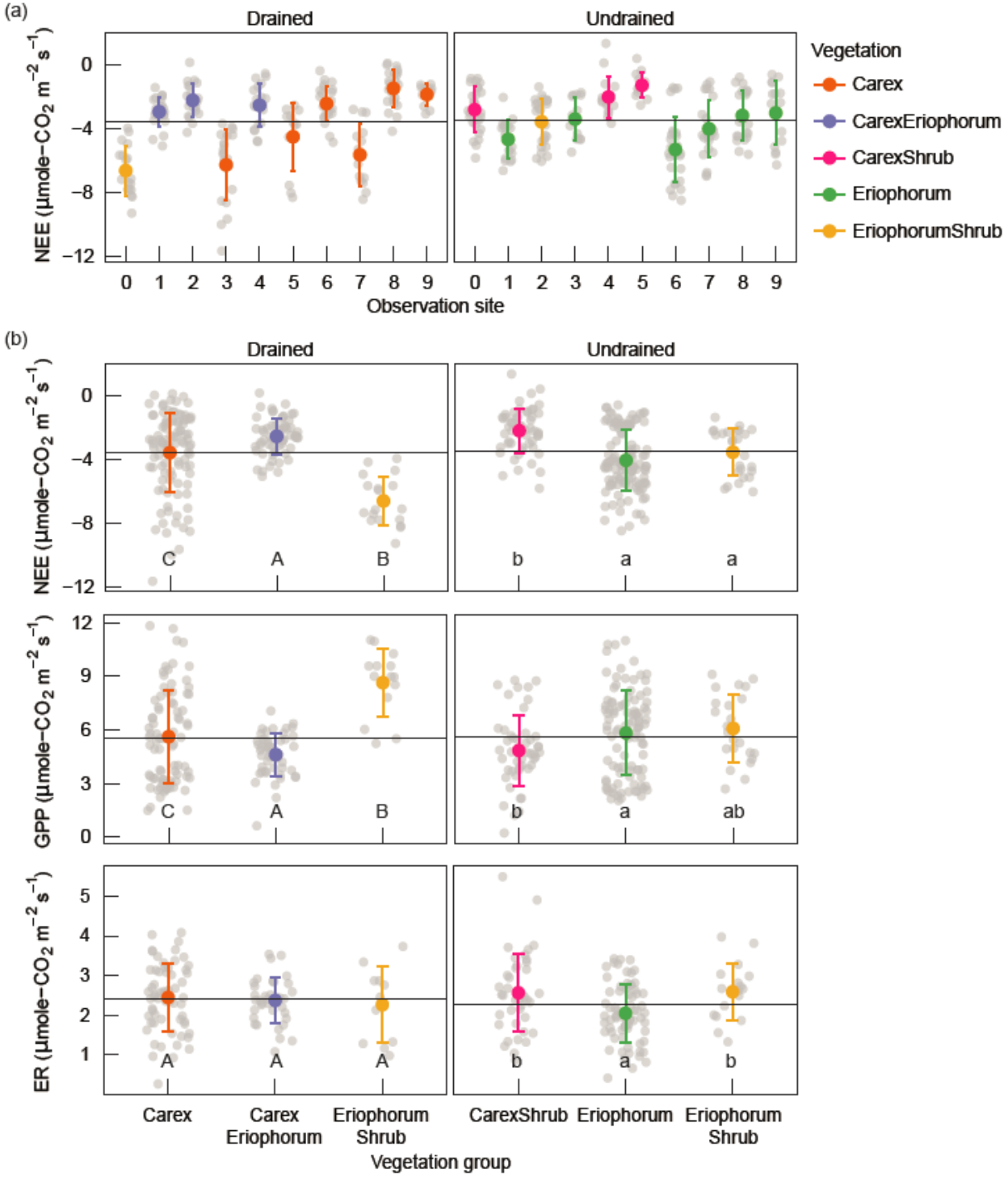

Biogeosciences Discuss., doi:10.5194/bg-2015-629, 2016
Manuscript under review for journal Biogeosciences
Published: 18 January 2016

Figure 7 (a) Variability of net ecosystem exchange (NEE) during the growing season of 2013 by vegetation type. Individual flux measurements are given as small gray points, and the colored points and error bars represent the mean flux rates and the standard deviations per observation site, with colors indicating the dominant vegetation species. The black horizontal bars show the mean flux rates averaged for the entire transect. (b) NEE (top), gross primary production (GPP, center), and ecosystem respiration (ER, bottom) rates aggregated by vegetation group. Significance of differences between groups, determined by one-way ANOVA and Tukey's post hoc test, is indicated by the letters. Different letters indicate significant difference among groups while the same letters indicate significant similarity.

Biogeosciences Discuss., doi:10.5194/bg-2015-629, 2016
Manuscript under review for journal Biogeosciences
Published: 18 January 2016

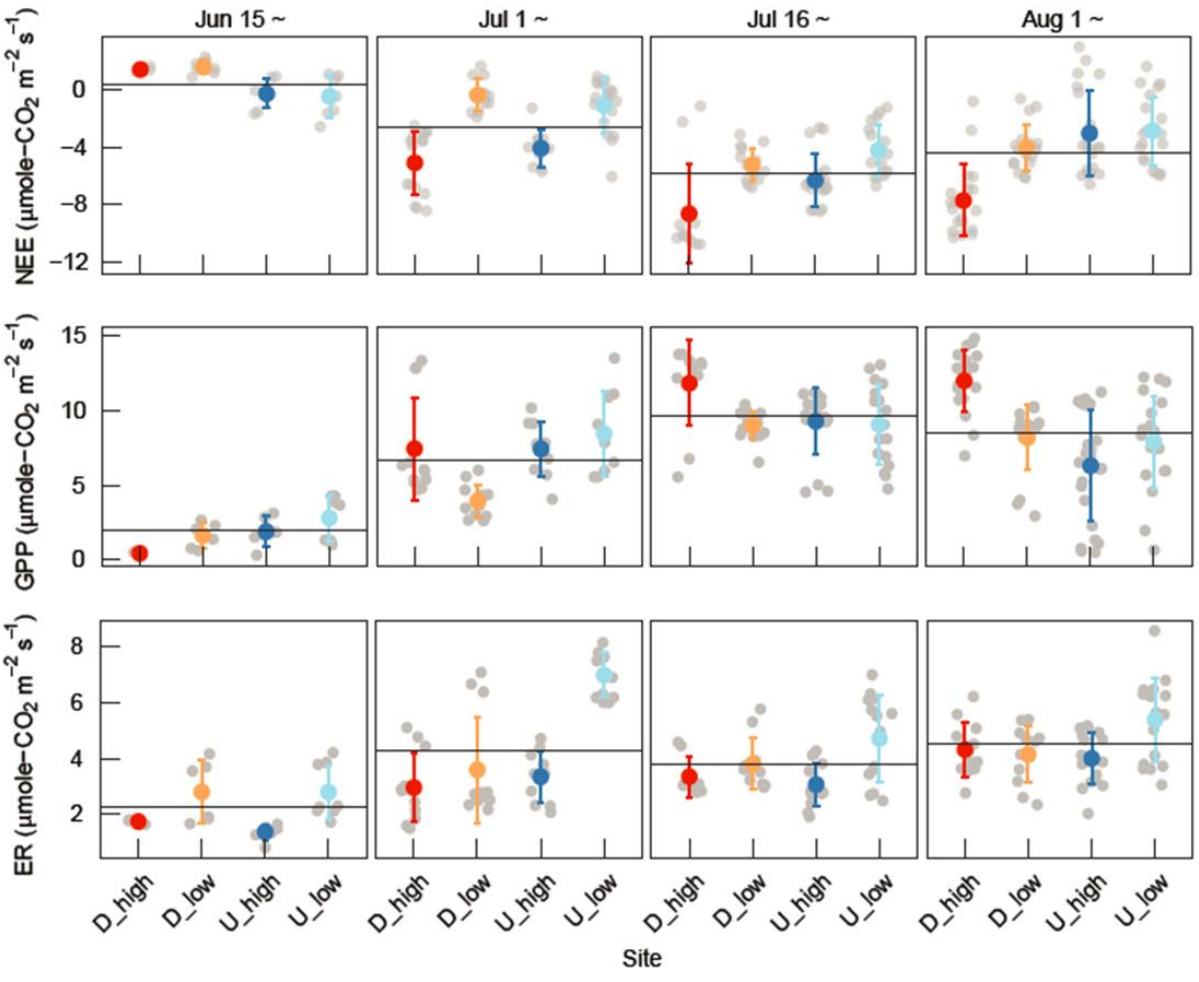

Figure 8 Net ecosystem exchange (NEE), gross primary production (GPP) and ecosystem respiration (ER) of the core sites over the growing season of 2014, divided into 4 sub-seasons with 15 days of interval starting from the
785 Jun 15. Individual flux measurements are given as small gray points, and colored points and error bars represent the mean flux rates and the standard deviations per observation site. The black horizontal bars show the mean flux rates averaged for the four sites by each sub-season.

Biogeosciences Discuss., doi:10.5194/bg-2015-629, 2016
Manuscript under review for journal Biogeosciences
Published: 18 January 2016

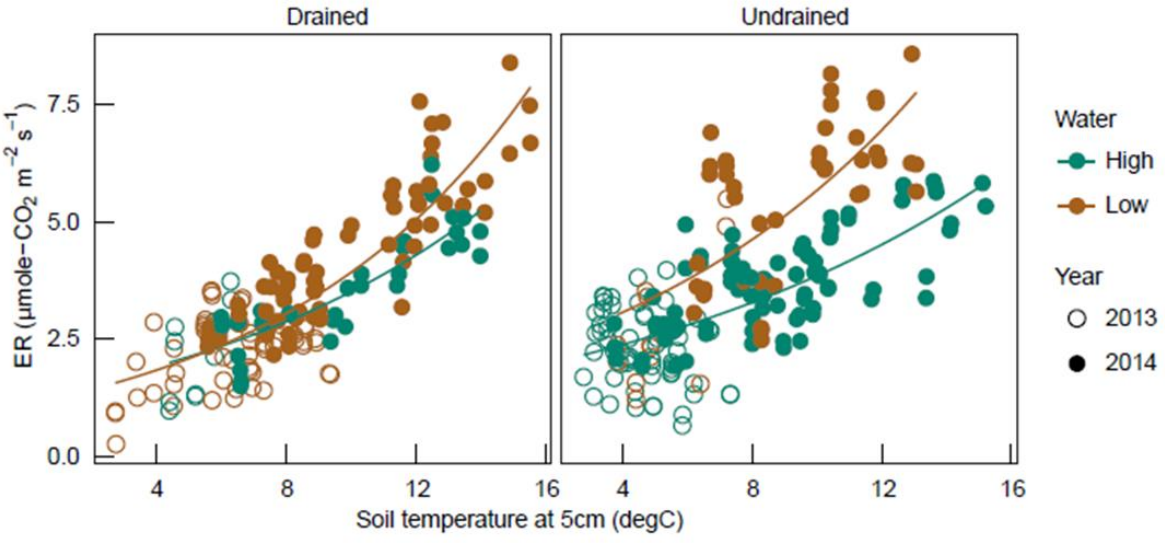

Figure 9 Relationships between soil temperatures at 5cm (X axis) and the rates of ecosystem respiration (ER, Y axis) by transect (columns) and water table depth (WTD) category (color). Data were separated by year (shape) and those from 2013 covered narrow ranges of soil temperatures compared to 2014 due to a shorter observation period.

Biogeosciences Discuss., doi:10.5194/bg-2015-629, 2016
Manuscript under review for journal Biogeosciences
Published: 18 January 2016

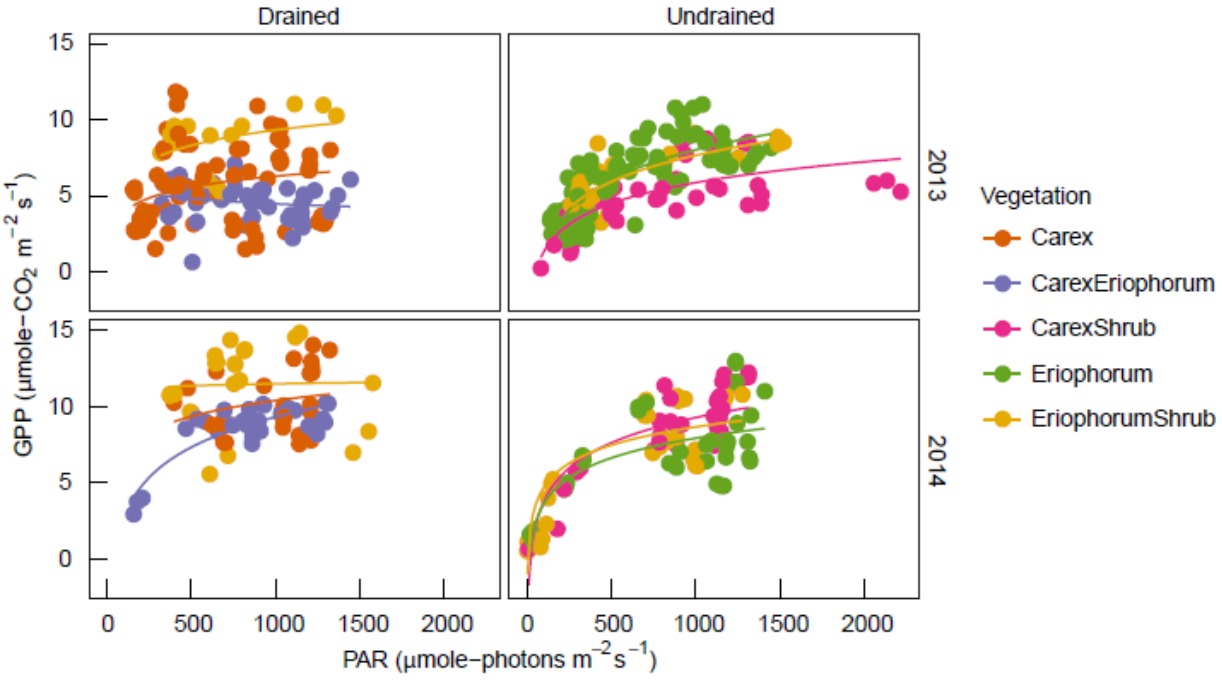

Figure 10 Logarithmic relations between photosynthetically active radiation (PAR, X axis) and gross primary production (GPP, Y axis) by transect (columns), vegetation type (color) and year (rows). Data points are only from August when vegetation activities were high to minimize seasonality.

Biogeosciences Discuss., doi:10.5194/bg-2015-629, 2016
Manuscript under review for journal Biogeosciences
Published: 18 January 2016

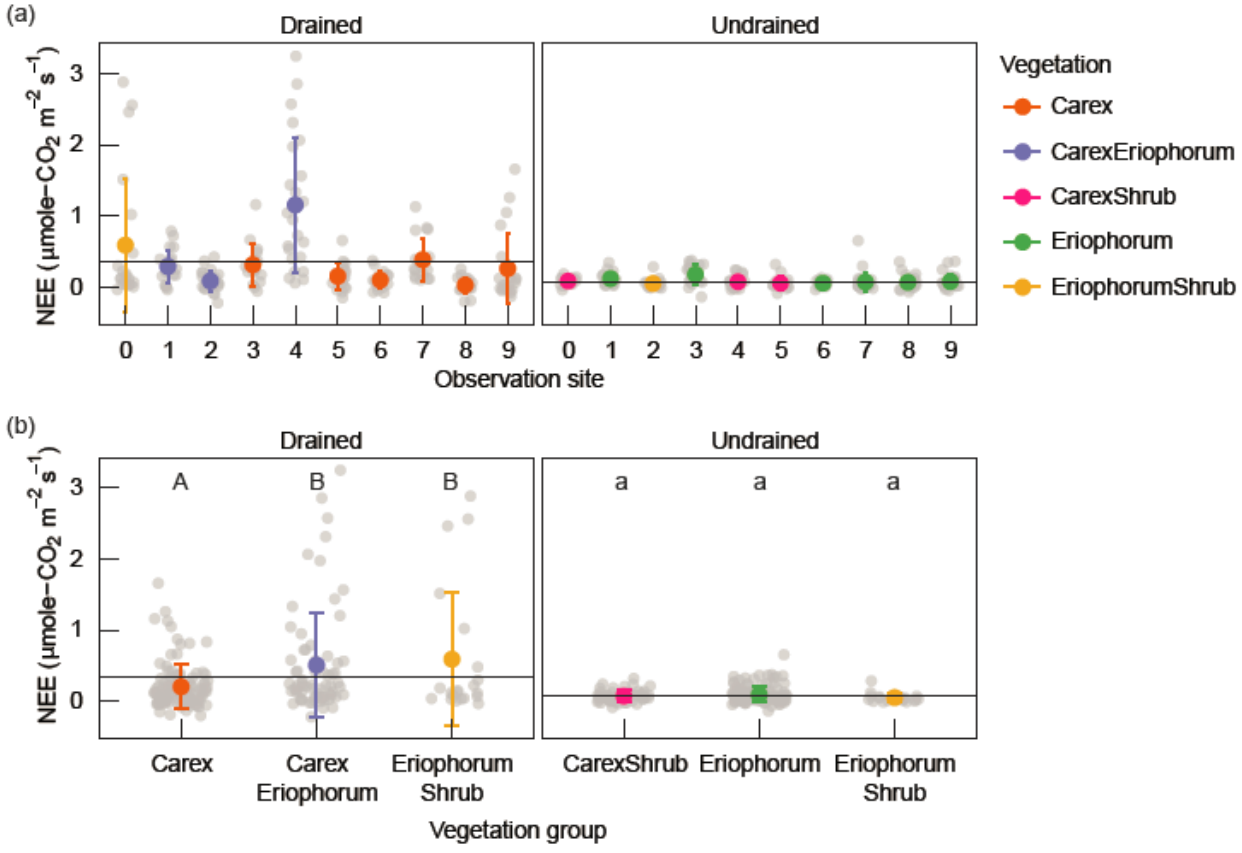

Figure 11 (a) Variability of net ecosystem exchange (NEE) across the transects in November 2013 by vegetation type (color). Individual flux measurements are given as small gray points, and the colored points and error bars represent the mean flux rates and the standard deviations per observation site. The black horizontal bars show the mean flux rates averaged for the entire transect. (b) Aggregated fluxes by vegetation type (color). Significance of differences between groups, determined by one-way ANOVA and Tukey's post hoc test, is indicated by the letters. Different letters indicate significant difference among groups while the same letters indicate significant similarity.

Biogeosciences Discuss., doi:10.5194/bg-2015-629, 2016
Manuscript under review for journal Biogeosciences
Published: 18 January 2016

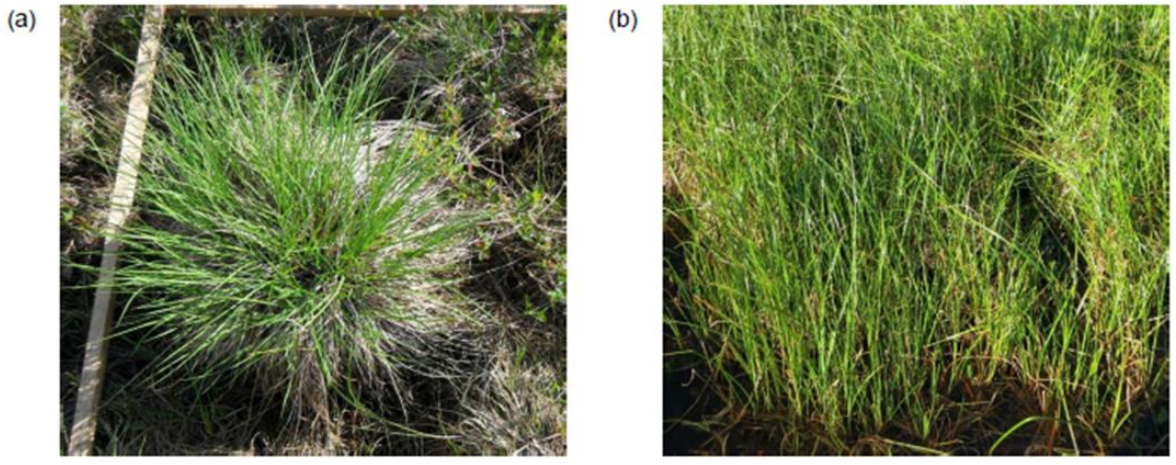

805 Appendix 1 The two most dominant vegetation species, (a) *Carex* species, (b) *Eriophorum angustifolium*

Biogeosciences Discuss., doi:10.5194/bg-2015-629, 2016
Manuscript under review for journal Biogeosciences
Published: 18 January 2016

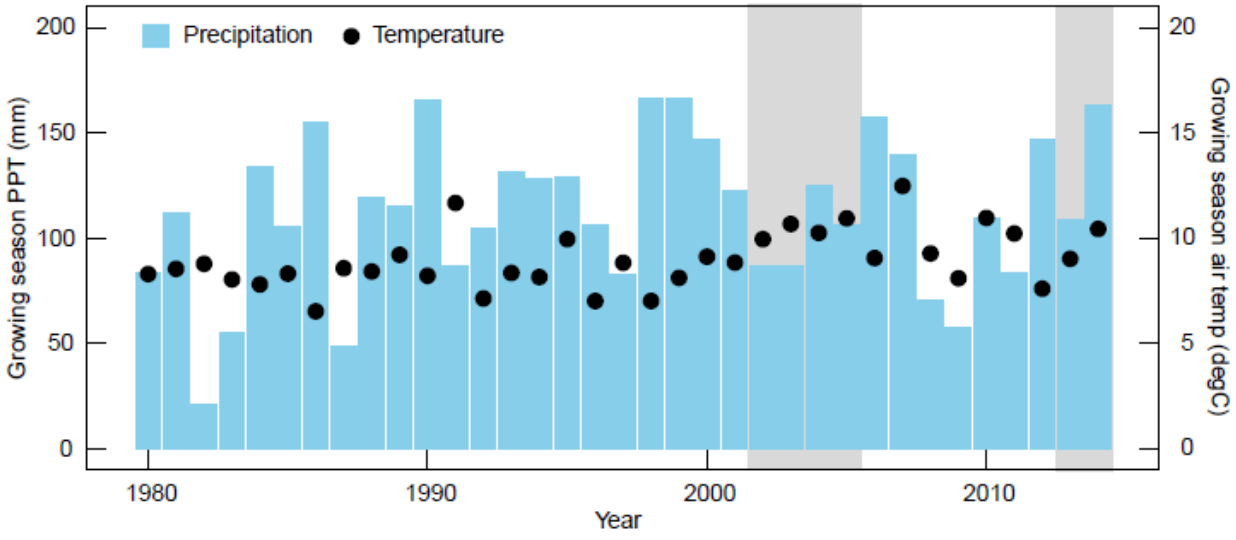

Appendix 2 Variability in growing-season (June to September) air temperatures (black points) and precipitation (blue bars) since 1980, based on the records of the Chersky weather station (68° 45' N, 161° 20' E, elevation: 31 m amsl, data retrieved from Reliable Prognosis). Shaded areas highlight the years with CO_2 flux measurements.

Biogeosciences Discuss., doi:10.5194/bg-2015-629, 2016
Manuscript under review for journal Biogeosciences
Published: 18 January 2016

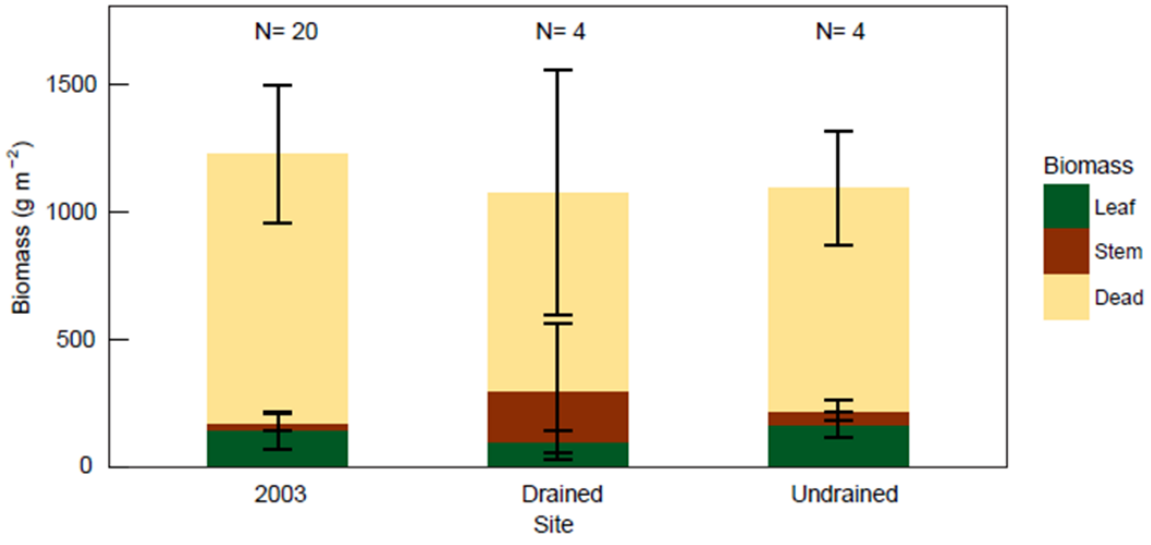

Appendix 3 The total aboveground dry biomass of standing dead and living plants, measured in 2003 (N = 20) and 2013 (N = 4). Weights of dry biomass were summed up regardless of species. Dead: standing dead materials largely from *Carex* species and *Eriophorum angustifolium*, stem: stems mainly from shrub species, leaf: green leaves of all species. The mean and the standard deviation values of replicates are described with bars and error bars.

Biogeosciences Discuss., doi:10.5194/bg-2015-629, 2016
Manuscript under review for journal Biogeosciences
Published: 18 January 2016

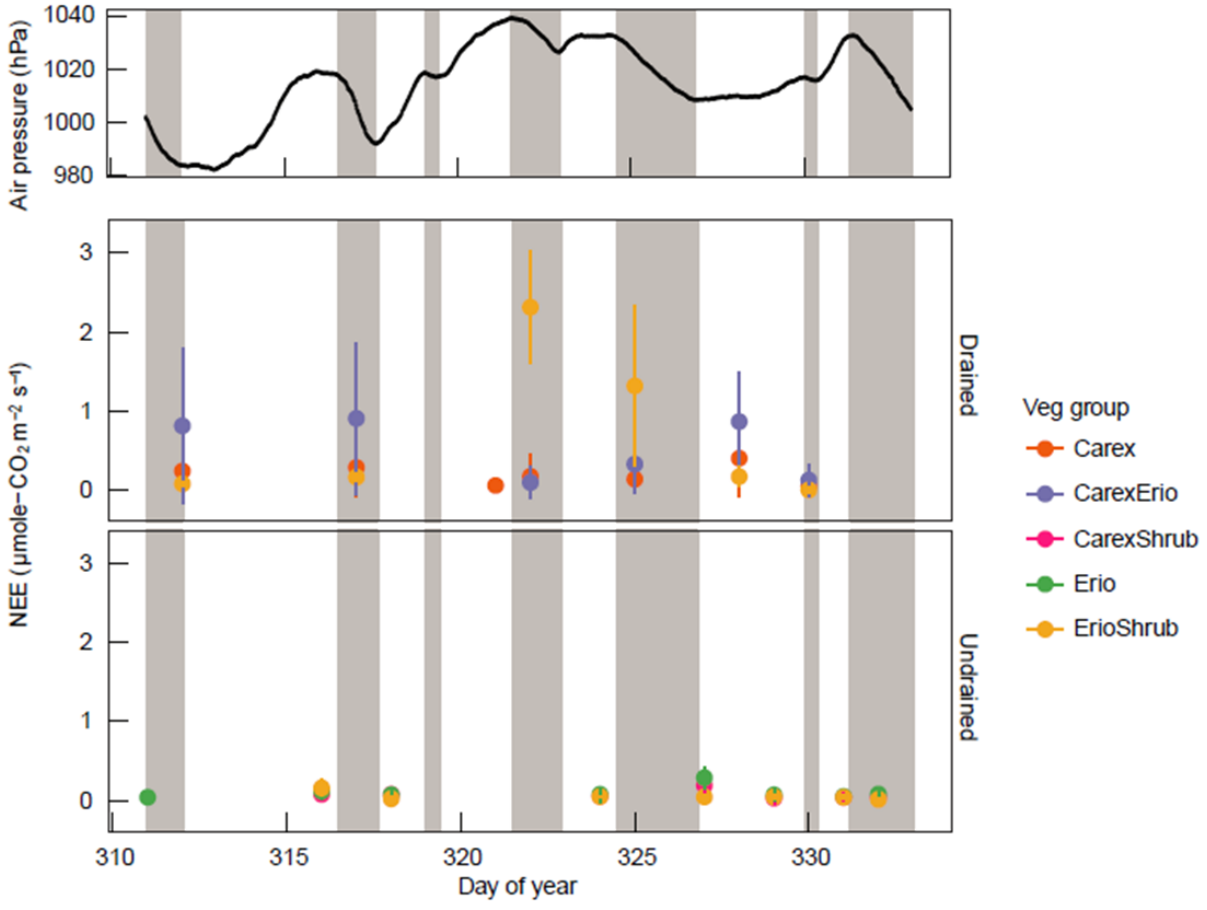

Appendix 4 Atmospheric pressure (top) and net ecosystem exchange (NEE) of November 2013 by vegetation type (color) presented in parallel. Time periods with decreasing air pressure were shaded in gray. NEE fluxes were pooled by vegetation group (color) and the mean values and the standard deviations were plotted.